Lepton-nucleus Scattering in Quasi-elastic Region

Kyungsik Kim

Korea Aerospace University

2021 nuclear summer school

Outlines:

1. Introduction

2. The Electron Scattering Theory

3. The Quasi-elastic Electron Scattering

4. The Neutrino-nucleus scattering

5. Appendix

I. Introduction

1.1 Historical Remarks

- In 1928, Dirac published his famous paper in which the Driac equation of the relativistic electron was given.
- One year later, Mott gave the theoretical derivation of the cross section for the relativistic scattering of Dirac particles by point nuclei, known as the "Mott formula".
- The pioneering experimental studies were begun in 1953 by Hofstadter *et al.* at the Stanford University Linear Accelerator (SLAC) with electrons of 116 MeV energy.
- The second phase at the Stanford studied the charge and magnetic moment distributions of single nucleons by elastic electron scattering.
- The third phase with higher-current is the study of the complex nuclei up to 600 MeV at Saclay in later 1960's.
- After that, several accelerators were built such as MIT Bates with 1 GeV energy, JLab, and so on.
- The neutron skin depth was measured by using electron parity violation off ^{208}Pb and ^{40,48}Ca at JLab.
- Measured the neutrino-proton and antineutrino-proton elastic scattering at BNL on the middle of 80's.

- Measured the neutrino (antineutrino) neutral (charged)-current quasi-elastic differential cross sections at MiniBooNE from 2010 to 2015 and then obtained axial mass $M_A = 1.30$ GeV and strange quark form factor $\Delta s = 0.08$ at $Q^2 = 0$.

- The axial mass $M_A = 0.99$ GeV was obtained from antineutrino charge-current reaction on hydrocarbon at MINERνA.

- The axial mass $M_A = 1.23$ GeV was obtained from neutrino charge-current reaction on iron at MINOS.

- The axial mass $M_A = 1.26$ GeV was obtained from neutrino charge-current reaction on iron at T2K.

- Recently neutrino charged-current quasi-elastic scattering with monoenergetic muon neutrino at 236 MeV by using kaon-decays-at rest(KDAR: $K^+ \to \mu^+ + \nu_\mu$) at MiniBooNE.

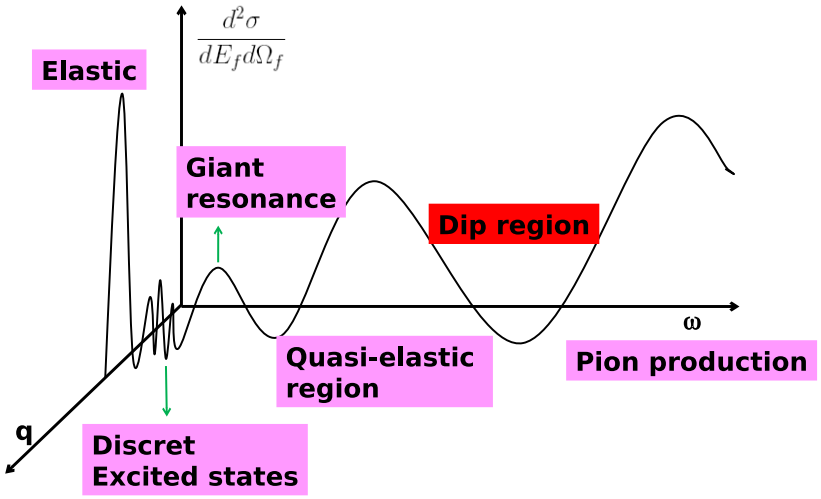

FIG. 1: Region in terms of energy transfer at fixed three momentum transfer.

1.2 General Features of lepton Scattering

Different electron scattering processes depending on energy transfer ω as shown in Fig. 1:

- A large peak at $\omega = 0$ produced by elastic scattering from the charge distribution in the nuclear ground state.
- Peaks due to the excitation of discrete levels below the particle emission threshold occur as the energy transfer ω increases.
- Overlapping peaks with several MeV width caused by excitation of collective models, so called "giant resonances".
- The quasi-elastic peak, where a nucleon is directly knocked out of the nucleus by the electromagnetic field of the passing electrons. The width

of the peak, which is dependent on kinematics condition, is a consequence of the internal motion of the nucleon inside the nucleus, referred to "Fermi motion".

- Broad peak which corresponds to pion production processes where the energy transfer is large enough to excite the individual nucleon.

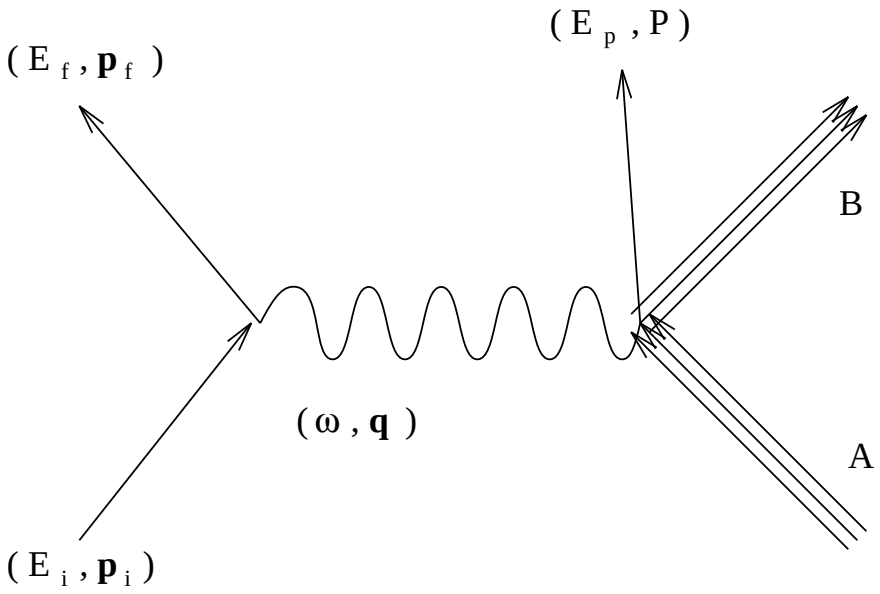

FIG. 2: Kinematics for the electron-nucleus scattering

II. The Electron Scattering Theory

2.1 The Dirac Equation

The Dirac equation for a single-particle in a spherically symmetric potential $V(r)$ is given by

$$\{\boldsymbol{\alpha}\cdot\mathbf{p} + \beta m + V(r)\}\Psi(\mathbf{r}) = E\Psi(\mathbf{r}) \tag{1}$$

where m is the mass of the particle, $\boldsymbol{\alpha}$ and β are the standard 4×4 Dirac matrices and $\Psi(\mathbf{r})$ is the four element wave function. The wave function can be separated into an angle-dependent part and a radial part via a partial wave expansion.

When there is no potential, the solution has the well known plane wave

form given by

$$\Psi(\mathbf{r}) = \sqrt{\frac{E+m}{2E}} \begin{pmatrix} I \\ \frac{\boldsymbol{\sigma}\cdot\mathbf{p}}{E+m} I \end{pmatrix} e^{i\mathbf{p}\cdot\mathbf{r}} \chi_s \tag{2}$$

where I represents a 2×2 unit matrix and $\boldsymbol{\sigma}$ contains the 2×2 Pauli matrices. The notation χ_s with $s = \pm\frac{1}{2}$ is the Pauli two component spinors. For spin-$\frac{1}{2}$, the eigenfunction of total angular momentum $\mathbf{J} = \mathbf{L} + \frac{1}{2}\boldsymbol{\sigma}$ is represented by the spin angle function:

$$\chi_\kappa^\mu(\hat{r}) = \sum_{m,s} \langle lm, \frac{1}{2} s | j\mu \rangle Y_l^m(\hat{r}) \chi_s \tag{3}$$

where $\kappa = \pm(j + \frac{1}{2})$ is an eigenvalue of the operator $\mathbf{K} = \beta(\boldsymbol{\sigma}\cdot\mathbf{L} + 1)$, and is given by

$$\kappa = \begin{pmatrix} l & \text{for} & j = l - \frac{1}{2} \\ -l-1 & \text{for} & j = l + \frac{1}{2}. \end{pmatrix}$$

Here, κ takes on all positive and negative integer values except zero. The κ value specifies both the total angular momentum quantum number j and the orbital angular momentum quantum number l

$$l = \begin{pmatrix} \kappa & \text{for} & \kappa > 0 \\ -\kappa - 1 & \text{for} & \kappa < 0 \end{pmatrix} \tag{4}$$

and $j = |\kappa| - \frac{1}{2}$.

By using the Rayleigh expansion, the exponential in the plane wave becomes

$$e^{i\mathbf{p}\cdot\mathbf{r}} = \sum_l (i)^l (2l+1) j_l(pr) P_l(\cos\Theta),$$

where Θ is the angle between $\hat{p}$ and $\hat{r}$. Using the addition theorem of the

spherical harmonics, this becomes

$$e^{i\mathbf{p}\cdot\mathbf{r}} = \sum_{lm} 4\pi(i)^l j_l(pr) Y_l^{m*}(\hat{p}) Y_l^m(\hat{r}). \tag{5}$$

Multiply Eq. (5) by spinor χ_s and substitute the spin angle function of Eq. (3) to obtain

$$\begin{aligned} e^{i\mathbf{p}\cdot\mathbf{r}}\chi_s &= \sum_{lm} 4\pi(i)^l j_l(pr) Y_l^{m*}(\hat{p}) Y_l^m(\hat{r})\chi_s \\ &= \sum_{\kappa,\mu,m} 4\pi(i)^l j_l(pr) Y_l^{m*}(\hat{p}) \langle lm, \frac{1}{2}s|j\mu\rangle \chi_\kappa^\mu(\hat{r}). \end{aligned} \tag{6}$$

By using Eq. (6), we finally obtain the the partial wave form for the plane wave

$$\Psi(\mathbf{r}) = \sqrt{\frac{E+m}{2E}} \sum_{\kappa\mu} 4\pi(i)^l \langle l\mu - s, \frac{1}{2}s|j\mu\rangle \psi_\kappa^\mu(\mathbf{r}), \tag{7}$$

where

$$\psi_\kappa^\mu(\mathbf{r}) = \begin{pmatrix} j_l(pr)\chi_\kappa^\mu(\hat{r}) \\ \frac{is_\kappa p}{E+m} j_{\bar{l}}(pr)\chi_{-\kappa}^\mu(\hat{r}) \end{pmatrix} \tag{8}$$

and we have introduced $\bar{l} = l(-\kappa)$ and defined $s_\kappa = \text{sign}(\kappa) = l - \bar{l}$. Therefore,

$$\begin{aligned} (\boldsymbol{\sigma}\cdot\mathbf{L} + 1)\chi_\kappa^\mu(\hat{r}) &= -\kappa\chi_\kappa^\mu(\hat{r}) \\ \sigma_r\chi_\kappa^\mu(\hat{r}) &= -\chi_\kappa^\mu(\hat{r}), \end{aligned} \tag{9}$$

where $\sigma_r = \boldsymbol{\sigma}\cdot\hat{r}$ is a scalar operator so that $\sigma_r\chi_\kappa^\mu$ belongs to the same j and μ values.

For any spherically symmetric potential $V(r)$, the radial part of the wave function can be separated with the angular function and then, the wave function can be defined by

$$\psi_\kappa^\mu(\mathbf{r}) = R_\kappa(r)\chi_\kappa^\mu(\hat{r}) \tag{10}$$

where the radial function R is written by

$$R_\kappa(r) = \begin{pmatrix} f_\kappa(r) \\ ig_\kappa(r) \end{pmatrix}. \tag{11}$$

The radial equation can be written as

$$\begin{aligned} \frac{df}{dr} &= -\frac{\kappa+1}{r} f(r) + [m + E - V(r)]g(r) \\ \frac{dg}{dr} &= \frac{\kappa-1}{r} g(r) + [m - E + V(r)]f(r). \end{aligned} \tag{12}$$

For a spherically symmetric potential, the wave function has the same form as the plane wave but one needs the phase shift due to the potential. The distorted wave functions for the electrons are obtained by solving the Dirac equation in the presence of the static Coulomb potential of the nuclear charge distribution. The Coulomb distorted incoming electron wave function can be written as a summation of the partial waves, for incoming spin s_i, as

$$\Psi_i^{s_i}(\mathbf{r}) = \sum_{\kappa_i \mu_i} C_{\kappa_i \mu_i} e^{i\delta_{\kappa_i}} \psi_{\kappa_i}^{\mu_i}(\mathbf{r}). \tag{13}$$

The outgoing electron wave function for outgoing spin s_f is given by

$$\Psi_f^{s_f}(\mathbf{r}) = \sum_{\kappa_f \mu_f} C_{\kappa_f \mu_f} e^{-i\delta_{\kappa_f}} \psi_{\kappa_f}^{\mu_f}(\mathbf{r}). \tag{14}$$

In Eq. (13) and Eq. (14), $\psi_\kappa^\mu(\mathbf{r})$ is the electron eigenstate with angular momentum quantum number κ, μ given by

$$\psi_\kappa^\mu(\mathbf{r}) = \begin{pmatrix} f_\kappa(r)\chi_\kappa^\mu(\hat{r}) \\ ig_\kappa(r)\chi_{-\kappa}^\mu(\hat{r}) \end{pmatrix} \tag{15}$$

where $\chi_\kappa^\mu(\hat{r})$ is the same as the Eq. (3) and the radial functions $f(r)$ (or $g(r)$) are obtained by solving numerically the two coupled Dirac radial equations.

To satisfy the incoming (or outgoing) boundary condition, we need

$$C_{\kappa\mu} = \sqrt{\frac{E+m}{2E}} 4\pi (i)^l \langle l\ \mu - s\ , \frac{1}{2} s | j\mu \rangle Y_l^{\mu - s^*}(\hat{p}). \tag{16}$$

δ_κ is the phase shift for the partial wave, m is the electron mass, and s is the electron spin projection.

2.2 Phase Shift Analysis for Relativistic Coulomb Wave Functions

In order to evaluate the phase shift of the continuum state wave functions, we solve the radial wave function for a point charge Coulomb potential (V(r)=-$\frac{\alpha Z}{r}$). The two coulped radial equations for the point Coulomb potential are

$$\begin{aligned} \frac{d}{dr} f^c &= -\frac{\kappa+1}{r} f^c + (m + E + \frac{\alpha Z}{r}) g^c \\ \frac{d}{dr} g^c &= \frac{\kappa-1}{r} g^c + (m - E + \frac{\alpha Z}{r}) f^c \end{aligned} \tag{17}$$

where $\alpha = e^2 = \frac{1}{137}$ is the fine-structure constant and Z is the atomic(charge) number. The superscript c denotes the point Coulomb potential.

As usual, there are two independent solutions. One is a regular solution which is finite at the origin, the other is the irregular solution. The solutions can be written in terms of the Whittaker functions $M_{\lambda,\mu}(z)$:

$$\begin{aligned} f^c &= \sqrt{\frac{E+m}{4pE}} \exp(\frac{\pi\eta}{2}) \frac{|\Gamma(\nu+1-i\eta)|}{\Gamma(2\eta+1)} (r^{-\frac{3}{2}}) \\ &\times \mathrm{Re}[\exp(-\frac{i\pi}{2}(\nu+\frac{1}{2}) + i\phi) M_{-i\eta+\frac{1}{2},\nu}(2ipr)] \end{aligned} \tag{18}$$

$$\begin{aligned} g^c &= \sqrt{\frac{E-m}{4pE}} \exp(\frac{\pi\eta}{2}) \frac{|\Gamma(\nu+1-i\eta)|}{\Gamma(2\eta+1)} (r^{-\frac{3}{2}}) \\ &\times \mathrm{Im}[\exp(-\frac{i\pi}{2}(\nu+\frac{1}{2}) + i\phi) M_{-i\eta+\frac{1}{2},\nu}(2ipr)], \end{aligned} \tag{19}$$

where Re means the real part of [...] and Im means the imaginary part of [...]. The constants ν and η are given by

$$\nu = \pm\sqrt{\kappa^2 - (\alpha Z)^2} \tag{20}$$

$$\eta = \frac{\alpha Z E}{p} \tag{21}$$

and the phase ϕ becomes

$$e^{2i\phi} = -\frac{\kappa + i\eta\frac{m}{E}}{\nu + i\eta}. \tag{22}$$

The Whittaker function for $r\to 0$ becomes

$$M_{\lambda,\mu}(z) \approx e^{-\frac{z}{2}} z^{\nu+\frac{1}{2}}. \tag{23}$$

The asymptotic form at $r\to\infty$ is given by

$$f^c \approx \sqrt{\frac{E+M}{4pE}}(\frac{1}{r})\,\cos\left[pr - (l+1)\frac{\pi}{2} + \eta \ln(2pr) + \delta_\kappa^c\right] \tag{24}$$

$$g^c \approx -\sqrt{\frac{E-M}{4pE}}(\frac{1}{r})\,\sin\left[pr - (l+1)\frac{\pi}{2} + \eta \ln(2pr) + \delta_\kappa^c\right]. \tag{25}$$

The regular solution needs the positive value $\nu > 0$ and the irregular solutions needs the negative value $\nu < 0$.

In the asymptotic region, the radial wave functions in the presence of a short range additional potential can be written in terms of a linear combination of the regular and the irregular solutions for point charge Coulomb functions

$$\begin{aligned} f &= A f_R^c + B f_I^c \\ g &= A g_R^c + B g_I^c, \end{aligned} \tag{26}$$

where the subscript R (or I) denotes the regular (or irregular) solution. The solutions have the following asymptotic forms as $r\to\infty$

$$f\approx\sqrt{\frac{E+M}{4pE}}(\frac{1}{r})\cos\left[pr-(l+1)\frac{\pi}{2}+\eta\ln\left(2pr\right)+\delta_\kappa^c+\delta_\kappa\right] \tag{27}$$

$$g\approx-\sqrt{\frac{E-M}{4pE}}(\frac{1}{r})\sin\left[pr-(l+1)\frac{\pi}{2}+\eta\ln\left(2pr\right)+\delta_\kappa^c+\delta_\kappa\right]. \tag{28}$$

The coefficients A and B and the additional phase δ_κ are given by

$$A=\frac{f_I^c g-g_I^c f}{f_I^c g_R^c-f_R^c g_I^c} \tag{29}$$

$$B=\frac{g_R^c f-f_R^c g}{f_I^c g_R^c-f_R^c g_I^c} \tag{30}$$

and

$$\tan\delta_\kappa=\frac{\sin\theta}{\frac{A}{B}+\cos\theta} \tag{31}$$

where

$$\theta=\delta_{\kappa,I}^c-\delta_{\kappa,R}^c.$$

The phase difference θ between the regular and irregular point Coulomb function must be nonzero and gives imprecise values of δ_κ if θ is too small.

For $m_e\to0$, the radial functions become

$$f_{-\kappa}=g_\kappa\qquad,\qquad g_{-\kappa}=f_\kappa,$$

and the phase shift is

$$\delta_{-\kappa}=\delta_\kappa.$$

We found the regular and the irregular Coulomb wave functions for the negatively charged particle in the Coulomb field. For a positively charged particle

such as a proton, the Coulomb wave functions can be obtained by changing the sign of the charge value Z.

2.3 Relativistic Nucleon Wave Functions

The most general time-independent local Dirac equation containing the five Lorentz-covariant interaction of Dirac theory can be written as

$$\begin{aligned}&\{\boldsymbol{\alpha}\cdot\mathbf{p}+\beta[m+U_S(\mathbf{r})+\gamma_\mu U_V^\mu(\mathbf{r})+\gamma_5 U_{PS}(\mathbf{r})\\&+\gamma_\mu\gamma_5 U_{PV}(\mathbf{r})+\sigma_{\mu\nu}U_T^{\mu\nu}(\mathbf{r})]\}\Psi(\mathbf{r})=E\Psi(\mathbf{r})\end{aligned}\tag{32}$$

where $\boldsymbol{\alpha}$, β, γ_μ, γ_5 and $\sigma_{\mu\nu}$ are the 4×4 Dirac matrices. The potential subscripts S, V, PS, PV and T represent scalar, vector, pseudoscalar, pseudovector and tensor, respectively. The requirement that the parity and the angular momentum operators commute with each term of the Hamiltonian in Eq. (32) introduces simplifying restrictions upon the interactions, e.g., $U_{PS}(\mathbf{r})$ and $U_{PV}(\mathbf{r})$ become zero. By applying these restrictions to the scalar term in the Hamiltonian, the function $U_S(\mathbf{r})$ is independent of angle. The contraction of vector potential and tensor potential can be expressed as

$$\begin{aligned}\gamma_\mu U_V^\mu(\mathbf{r}) &= \gamma_0 U_V^0(\mathbf{r})-\boldsymbol{\gamma}\cdot\mathbf{U}_V(\mathbf{r})=\gamma_0 U_V^0(\mathbf{r})-\gamma^r U_V^r(\mathbf{r})\\ \sigma_{\mu\nu}U_T^{\mu\nu}(\mathbf{r}) &= -\gamma^0\boldsymbol{\gamma}\cdot\mathbf{U}_T(\mathbf{r})=-\gamma^0\gamma^r U_T^r(\mathbf{r}).\end{aligned}$$

The Eq. (32) becomes

$$\{\boldsymbol{\alpha}\cdot\mathbf{p}+\beta[m+U_S(\mathbf{r})+\gamma_0 U_V^0(\mathbf{r})-\gamma^r U_V^r(\mathbf{r})-\gamma^0\gamma^r U_T^r(\mathbf{r})]\}\Psi(\mathbf{r})=E\Psi(\mathbf{r}).\tag{33}$$

The scalar and zeroth term of the vector potential must be rotationally invariant and thus every term become only a function of the magnitude of

the variable r. For local and time-independent interactions, hermiticity and time reversal invariance require $U_T^r(\mathbf{r})$ to be pure imaginary. However, since hermiticity requires $U_V^r(\mathbf{r})$ to be real while time reversal invariance requires it to be imaginary it vanishes. One must choose appropriate scalar and vector potentials that provide the dominant central and spin orbit interactions to obtain elastic scattering observables. These are referred to as the scalar potential $U_S(\mathbf{r}) = S(\mathbf{r})$, the vector potential $U_V(\mathbf{r}) = V(\mathbf{r})$, and is called the S-V model. Experiment requires that the potentials be large, several hundred MeV in strength, with the scalar attractive and the vector repulsive. By an extensive fitting to the experimental data the S-V model is recommended over the others. The single particle wavefunction of good angular momentum $\mathbf{J}^2$, J_z, parity P and time reversal symmetry T in Eq. (33) has the following form

$$\Psi(\mathbf{r}) = \begin{pmatrix} f_\kappa(r)\chi_\kappa^\mu(\hat{r}) \\ ig_\kappa(r)\chi_{-\kappa}^\mu(\hat{r}) \end{pmatrix}. \tag{34}$$

The coupled radial differential equations can be written by

$$\begin{aligned} \frac{df_\kappa}{dr} &= -\frac{\kappa+1}{r}f_\kappa(r) + [m + E + S(r) - V(r)]g_\kappa \\ \frac{dg_\kappa}{dr} &= \frac{\kappa-1}{r}g_\kappa(r) + [m - E + S(r) + V(r)]f_\kappa(r). \end{aligned} \tag{35}$$

We can obtain the radial functions $f_\kappa(r)$ and $g_\kappa(r)$ by solving the two differential equations numerically. Fig. 3 shows that the radial wave function for $3s_{1/2}$ state of ^{208}Pb as an example.

Using the global optical potential, obtained from fitting elastic proton scattering data, the knocked-out proton can be described by scalar and vector potentials similar to the bound state potentials except that they contain an imaginary part to describe loss of flux from the elastic channel. The wave

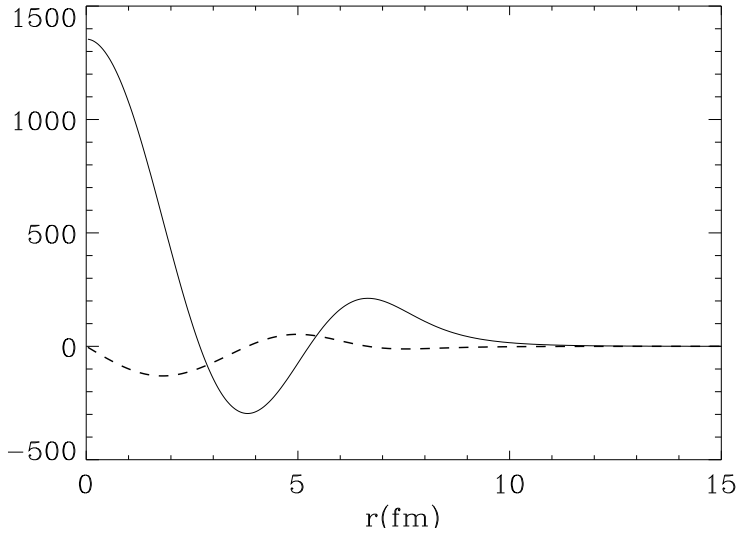

FIG. 3: Relativistic $3s_{1/2}$ wave function in ^{208}Pb. The solid line is f_κ and the dash line is g_κ.

function for the outgoing nucleon has the same structure as the outgoing electron wave function (14):

$$\Psi_{\rm p}(\mathbf{r}) = \sum_{\kappa_p \mu_p} C_{\kappa_p \mu_p} e^{-i\delta^*_{\kappa_p}} \psi^{\mu_p}_{\kappa_p}(\mathbf{r}) \tag{36}$$

where $\psi^{\mu_p}_{\kappa_p}(\mathbf{r})$ and $C_{\kappa_p \mu_p}$ are given by

$$\psi^{\mu_p}_{\kappa_p}(\mathbf{r}) = \begin{pmatrix} f^*_{\kappa_p}(r)\chi^{\mu_p}_{\kappa_p}(\hat{r}) \\ g^*_{\kappa_p}(r)\chi^{\mu_p}_{-\kappa_p}(\hat{r}) \end{pmatrix}$$

and

$$C_{\kappa_p \mu_p} = \sqrt{\frac{E_p + M}{2E_p}} 4\pi (i)^{l_p} \langle l_p \mu_p - s\, \frac{1}{2} s | j_p \mu_p \rangle Y^{\mu_p - s^*}_{l_p}(\hat{p})$$

and the $*$ denotes the complex conjugate.

III. The Quasi-elastic Electron Scattering

In our calculation, we make the following assumptions:

- The incoming and outgoing electrons are described by distorted wave function due to the nuclear static Coulomb potential of the target.
- The virtual photon emitted by the electron is absorbed by a single nucleon.
- The ejected nucleon interacts with the residual nucleus through a relativistic optical potential.
- The target nucleus is described by a relativistic independent particle model with the scalar and vector average potentials being determined in the Hartree approximation of the $\sigma - \omega$ model.

There are two processes: One is called the exclusive $(e, e'p)$ reaction by detecting simultaneously the final electron and the knocked-out nucleon. The other one is called the inclusive (e, e') reaction by detecting only the final electron.

3.1 Plane Wave Born Approximation (PWBA)

In PWBA, both the incoming and outgoing electrons are described by the plane wave solutions of the Dirac equation. The well-known transition matrix element from electrodynamics is given by

$$H_i = \int J_\mu A^\mu d^3r \tag{37}$$

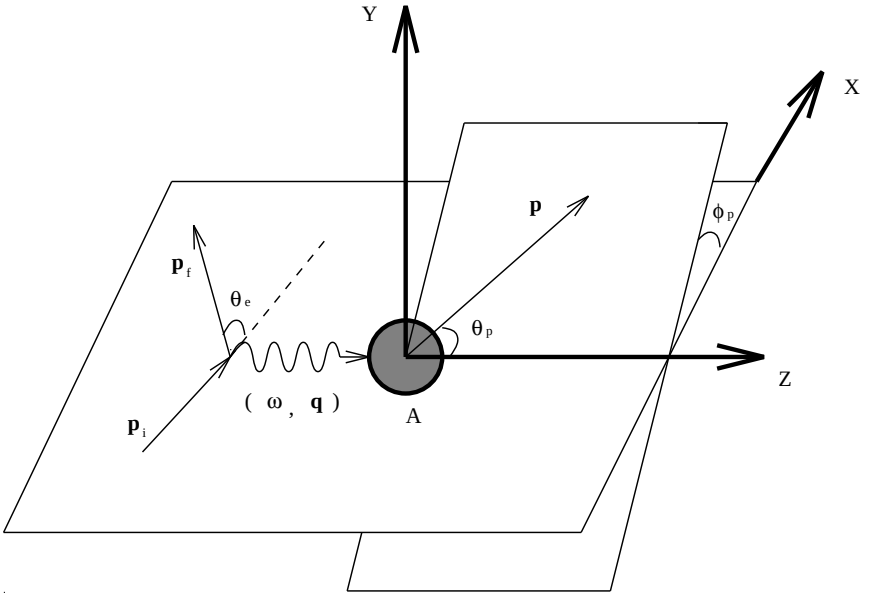

FIG. 4: Coordinate system.

where J_μ is the nuclear transition current and A^μ is the four potential generated by the electron current.

In the Lorentz gauge, the electron potential can be expressed in terms of the retarded Green function $G(\mathbf{r}', \mathbf{r})$ as

$$A^\mu(\mathbf{r}) = \int j^\mu(\mathbf{r}_e) G(\mathbf{r}_e, \mathbf{r}) d\mathbf{r}_e, \tag{38}$$

where

$$G(\mathbf{r}_e, \mathbf{r}) = \frac{e^{i\omega|\mathbf{r}_e - \mathbf{r}|}}{|\mathbf{r}_e - \mathbf{r}|}.$$

with the electron position vector $\mathbf{r_e}$, the nuclear position vector $\mathbf{r}$, and the energy loss ω. The electron current is given by

$$j^\mu = \bar{\psi}_f(\mathbf{r}_e)\gamma^\mu\psi_i(\mathbf{r}_e). \tag{39}$$

The electron four potential becomes the Möller potential:

$$\begin{aligned} A^\mu(\mathbf{r}) &= \frac{4\pi e}{q^2 - \omega^2} e^{i\mathbf{q}\cdot\mathbf{r}} \bar{u}(\mathbf{p}_f)\gamma^\mu u(\mathbf{p}_i) \\ &= e^{i\mathbf{q}\cdot\mathbf{r}} a^\mu, \end{aligned} \tag{40}$$

where $a^\mu = \frac{4\pi e}{q^2-\omega^2}\bar{u}(\mathbf{p}_f)\gamma^\mu u(\mathbf{p}_i)$ and the three momentum transfer $\mathbf{q} = \mathbf{p}_i - \mathbf{p}_f$. In terms of the Möller-type potential, the transition matrix element can be written as

$$H_i = a^\mu N_\mu \tag{41}$$

where the nuclear form factors can be defined in terms of the nuclear current density by

$$N_\mu = \int J_\mu(\mathbf{r}) e^{i\mathbf{q}\cdot\mathbf{r}} d^3r. \tag{42}$$

The nucleon transition current is given by

$$J_\mu(\mathbf{r}) = e\bar{\psi}_p \hat{J}_\mu \psi_b \tag{43}$$

where $\hat{J}_\mu$ is the nucleon current operator and ψ_b and ψ_p are the bound and continuum single particle wave function.

In PWBA, the nuclear form factor is just the Fourier transform of the current. The cross section for $(e, e'p)$ process can be written as

$$\frac{d^3\sigma}{dE_f d\Omega_f d\Omega_p} = \frac{1}{2}\frac{2\pi}{I_{in}}\rho_e\rho_p \sum_{s_i s_f s_p \mu_b} \frac{1}{2j_b+1}|H_i|^2 \tag{44}$$

where I_{in} is the incoming electron flux given by p_{in}/E_{in}. The s_i and s_f denote the initial and the final electron spin, and s_p and μ_b are the outgoing and the bound nucleon spin projections. The density of states ρ_e and ρ_p have the same form for outgoing electrons and nucleons and are given by the Fermi phase space as

$$\begin{aligned} d\mathbf{p} &= \rho dE d\Omega \\ \rho &= \frac{pE}{(2\pi)^3} \end{aligned} \tag{45}$$

where p and E are outgoing electron (nucleon) momentum and energy.

3.2 The Matrix element

In order to calculate the matrix element, we need to know the nucleon transition current which is given by

$$J_\mu(\mathbf{r}) = e\bar{\psi}_p \hat{J}_\mu \psi_b \tag{46}$$

where $\hat{J}_\mu$ is the nucleon current operator. For a free nucleon, the operator consists of two parts, namely, the Dirac contribution and the contribution of the anomalous magnetic moment μ_T:

$$\hat{J}^\mu = F_1\gamma^\mu + F_2\frac{i\mu_T}{2m_N}\sigma^{\mu\nu}q_\nu. \tag{47}$$

The charge density (zero component) and the three vector current are given by

$$\hat{J}^0 = F_1\gamma^0 + \frac{\mu_T}{2m_N}F_2\boldsymbol{\alpha}\cdot\mathbf{q} \tag{48}$$

$$\hat{J} = F_1\boldsymbol{\gamma} + \frac{\mu_T}{2m_N}F_2 q^0\boldsymbol{\alpha} + \frac{i\mu_T}{2m_N}F_2\boldsymbol{\Sigma}\times\mathbf{q} \tag{49}$$

where μ_T is the nucleon anomalous magnetic moment (for proton $\mu_T = 1.793$ and for neutron $\mu_T = -1.91$). Note $q^0 = \omega$ and $\mathbf{q}$ is an operator in configuration space. The nuclear form factors F_1 and F_2 are evaluated at four momentum transfer q_μ. They are related to the electric and magnetic form factors G_E and G_M by

$$G_E = F_1 + \frac{\mu_T q_\mu^2}{4M^2}F_2 \tag{50}$$

$$G_M = F_1 + \mu_T F_2. \tag{51}$$

We choose the standard result:

$$G_E = G_M/(\mu_T + 1) = (1 - q_\mu^2/0.71)^{-2} \tag{52}$$

where in this formula q_μ is in units of GeV. By using this current operator, the Fourier transform of the nucleon current density Eq. (42) can be written as

$$N_\mu = \int J_\mu(\mathbf{r}) e^{i\mathbf{q}\cdot\mathbf{r}} d^3r. \tag{53}$$

If we choose a well-defined $\mathbf{q}$, the longitudinal and transverse parts of the three vector current are defined by the following relations:

$$J_L \;=\; \mathbf{J}\cdot\hat{\mathbf{q}} \tag{54}$$

$$\mathbf{J}_T \;=\; \hat{\mathbf{q}}\times(\mathbf{J}\times\hat{\mathbf{q}}) \tag{55}$$

with

$$\mathbf{J} = \mathbf{J_L} + \mathbf{J_T}. \tag{56}$$

The current conservation for the nucleon and electron becomes $q^\mu J_\mu = q_\mu a^\mu = 0$. Using these relations, the transition matrix element becomes

$$\begin{aligned} H_i \;&=\; \int (a_0 J_0 - \mathbf{a}\cdot\mathbf{J}) e^{i\mathbf{q}\cdot\mathbf{r}} d^3r \\ &=\; \int [(1 - \frac{\omega^2}{q^2}) a_0 J_0 - \mathbf{a}\cdot\mathbf{J}] e^{i\mathbf{q}\cdot\mathbf{r}} d^3r \end{aligned} \tag{57}$$

and we can define the modified Fourier transform of the nucleon current density as a four vector in Eq. (53);

$$N^\mu = (N_0, N_x, N_y, 0) = (N_0, N_1, N_2, 0) \tag{58}$$

where

$$N_0 \;=\; \int -\frac{q_\mu^2}{q^2} J_0 e^{i\mathbf{q}\cdot\mathbf{r}} d^3r \tag{59}$$

$$N_x \;=\; \int J_x e^{i\mathbf{q}\cdot\mathbf{r}} d^3r \tag{60}$$

$$N_y \;=\; \int J_y e^{i\mathbf{q}\cdot\mathbf{r}} d^3r. \tag{61}$$

The cross section can be separated into the electron and nuclear components by defining an electron tensor (lepton tensor) in the conventional manner;

$$\eta^{\mu\nu} = \sum_{s_i s_f} [\bar{u}(p_f)\gamma^{\mu}u(p_i)]^*[\bar{u}(p_f)\gamma^{\nu}u(p_i)] \tag{62}$$

and a nuclear tensor (hadronic tensor);

$$W_{\mu\nu} = \sum_{s_p \mu_b} N_{\mu}^* N_{\nu}. \tag{63}$$

By using the relations, the cross section for $(e, e'p)$ reaction becomes

$$\begin{aligned}
\frac{d^3\sigma}{dE_f d\Omega_f d\Omega_p} &= \frac{1}{2}\frac{2\pi}{I_{in}}\rho_e\rho_p\frac{1}{2j_b+1}\sum_{s_i s_f s_P \mu_b}|H_i|^2 \\
&= \frac{1}{2}\frac{2\pi}{I_{in}}\rho_e\rho_p\frac{1}{2j_b+1}\sum_{s_i s_f s_P \mu_b}\frac{(4\pi\alpha)^2}{q_\mu^4}|\bar{u}(p_f)\gamma^{\mu}N_{\mu}u_(p_i)|^2 \\
&= \frac{1}{2}\frac{2\pi}{I_{in}}\rho_e\rho_p\frac{1}{2j_b+1}\frac{(4\pi\alpha)^2}{q_\mu^4}\sum_{s_i s_f s_P \mu_b}\eta^{\mu\nu}W_{\mu\nu}.
\end{aligned} \tag{64}$$

♦ Non-relativistic transition operator

Transition current operator is given by

$$J_{\mu}(q) = (\rho(q),\ \mathbf{J}(q)).$$

The charge and the vector parts are the Fourier transform of transition current:

$$\begin{aligned}
\rho(q) &= \int d\mathbf{r} e^{i\mathbf{q}\cdot\mathbf{r}}\langle f|\hat{\rho}(r)|i\rangle, \\
\mathbf{J}(q) &= \int d\mathbf{r} e^{i\mathbf{q}\cdot\mathbf{r}}\langle f|\hat{J}(r)|i\rangle
\end{aligned}$$

where the operators are given by

$$\hat{\rho}(r) = \sum_i e_i \delta(r - r_i),$$
$$\hat{J}(r) = \hat{J}_N(r) + \vec{\nabla} \times \hat{\mu}_N(r)$$

with

$$e_i = \frac{1}{2}(1 + \tau_3(i)),$$
$$\hat{J}_N(r) = \sum_i e_i \delta(r - r_i) \frac{\vec{\nabla}}{iM},$$
$$\hat{\mu}_N(r) = \sum_i \mu_i \frac{\sigma_i}{2M} \delta(r - r_i),$$
$$\mu_i = \frac{\mu_p + \mu_n}{2} - \frac{-\mu_p + \mu_n}{2} \tau_3.$$

Expand the partial wave

$$\hat{\rho}(r) = 4\pi \sum_{JM} Y^*_{JM}(\Omega_q) \langle f | \hat{M}^c_{JM} | i \rangle,$$
$$\hat{J}_\lambda(r) = -\sqrt{2\pi} \sum_{J \geq 1} \hat{J} \langle f | \hat{T}^E_{J\lambda} + \lambda \hat{T}^M_{J\lambda} | i \rangle$$

The c, E, and M denot the Coulomb, electric, and magnetic transitions given by

$$\hat{M}^c_{JM} = \int d^3r \; j_J(qr) i^J Y_{JM}(\Omega) \hat{\rho}(r),$$
$$\hat{T}^E_{J\lambda} = \frac{1}{q} \int d^3r \; \vec{\nabla} \times [j_J(qr) i^J Y^\lambda_{JJ1}] \cdot \hat{J}(r),$$
$$\hat{T}^M_{J\lambda} = \int d^3r \; j_J(qr) i^J Y^\lambda_{JJ1} \cdot \hat{J}(r).$$

The operator $\hat{J}$ is substituted into the above equation.

$$\hat{T}^E_{J\lambda} = \frac{1}{q} \int d^3r \; \{ [\vec{\nabla} \times j_J(qr) i^J Y^\lambda_{JJ1}] \cdot \hat{J}_N + [q^2 j_J(qr) i^J y^\lambda_{JJ1}] \cdot \hat{\mu}_N \},$$
$$\hat{T}^M_{J\lambda} = \int d^3r \; \{ [\vec{\nabla} \times j_J(qr) i^J Y^\lambda_{JJ1}] \cdot \hat{\mu}_N + [j_J(qr) i^J y^\lambda_{JJ1}] \cdot \hat{J}_N \}.$$

3.3 Inclusion of Electron Coulomb Distortion

Under the electron Coulomb distortion, the Rosenbluth in Eq. (64) is not valid any more and we need the multipole expansion. For the scalar terms, the Green function can be expanded as follows:

$$\begin{aligned} G(\mathbf{r},\mathbf{r}') &= \frac{e^{i\omega|\mathbf{r}-\mathbf{r}'|}}{|\mathbf{r}-\mathbf{r}'|} \\ &= 4\pi i\omega \sum_{LM} j_L(\omega r_<) h_L(\omega r_>) Y_L^M(\hat{r}) Y_L^{M^*}(\hat{r}'). \end{aligned} \tag{65}$$

For the vector current terms, one can expand the Green function with the Dyadic $\mathbf{I}$ in vector spherical harmonics:

$$\begin{aligned} \overleftrightarrow{G}(\mathbf{r},\mathbf{r}') &= \overleftrightarrow{I} G(\mathbf{r},\mathbf{r}') \\ &= 4\pi i\omega \sum_{JLM} j_L(\omega r_<) h_L(\omega r_>) \mathbf{Y}_{JL}^M(\hat{r}) \mathbf{Y}_{JL}^{M\,*}(\hat{r}'), \end{aligned} \tag{66}$$

where j_L and h_L denote the spherical Bessel and Hankel functions, respectively. The vector spherical harmonic function is defined as

$$\mathbf{Y}_{JL}^M(\hat{r}) = \sum_{\mu} \langle LM-\mu, 1\mu | JM\rangle Y_L^{M-\mu}(\hat{r})\hat{\xi}. \tag{67}$$

In terms of these definitions, the transition matrix element is written as:

$$\begin{aligned} H_i &= -4\pi i\omega \sum_{LM} \{ \int_0^\infty \rho^e Y_L^{M^*}(\hat{r}) [h_L(\omega r) \int_0^r \rho^N j_L(\omega r') Y_L^M(\hat{r}') d^3r' \\ &+ j_L(\omega r) \int_r^\infty \rho^N h_L(\omega r') Y_L^M(\hat{r}') d^3r'] d^3r \\ &- \sum_J \int_0^\infty \mathbf{j}\cdot\mathbf{Y}_{LJ}^{M\,*}(\hat{r}) [h_J(\omega r) \int_0^r \mathbf{J}\cdot\mathbf{Y}_{LJ}^M(\hat{r}') j_J(\omega r') d^3r' \\ &+ j_J(\omega r) \int_r^\infty \mathbf{J}\cdot\mathbf{Y}_{LJ}^M(\hat{r}') h_J(\omega r') d^3r'] d^3r \}. \end{aligned} \tag{68}$$

The scalar part of the nucleon current is given by

$$\int \bar{\psi}_p \hat{J}_0 \psi_b j_L(\omega r) Y_L^M(\hat{r}) d\Omega = \langle J_b\mu_b, LM | J_p\mu_p\rangle I_L(\kappa_p,\kappa_b) K_S^N(r), \tag{69}$$

where the radial integration $K_S(r)$ can be written as

$$\begin{aligned} K_S^N(r) &= F_1(f_{\kappa_p}f_{\kappa_b} + g_{\kappa_p}g_{\kappa_b})j_L(\omega r) + \frac{F_2\mu_T\omega}{2M}\frac{1}{2L+1} \\ &\times [(f_{\kappa_p}g_{\kappa_b} + g_{\kappa_p}f_{\kappa_b})((L+1)j_{L+1}(\omega r) - LJ_{L-1}(\omega r)) \\ &+ (\kappa_p - \kappa_b)(f_{\kappa_p}g_{\kappa_b} - g_{\kappa_p}f_{\kappa_b})(j_{L+1}(\omega r) + j_{L-1}(\omega r))]. \end{aligned} \tag{70}$$

The vector terms become

$$\begin{aligned} \int \bar{\psi}_p\hat{\mathbf{J}}\psi_b j_L(\omega r)\cdot\mathbf{Y}^M_{L\,L}(\hat{r})d\Omega &= \langle J_b\mu_b, LM|J_p\mu_p\rangle I_L(-\kappa_p,\kappa_b) \\ &\times K_V^N(r,\ L) \end{aligned} \tag{71}$$

$$\begin{aligned} \int \bar{\psi}_p\hat{\mathbf{J}}\psi_b j_L(\omega r)\cdot\mathbf{Y}^M_{L\,L-1}(\hat{r})d\Omega &= \langle J_b\mu_b, LM|J_p\mu_p\rangle I_L(\kappa_p,\kappa_b) \\ &\times K_V^N(r,\ L-1) \end{aligned} \tag{72}$$

$$\begin{aligned} \int \bar{\psi}_p\hat{\mathbf{J}}\psi_b j_L(\omega r)\cdot\mathbf{Y}^M_{L\,L+1}(\hat{r})d\Omega &= \langle J_b\mu_b, LM|J_p\mu_p\rangle I_L(\kappa_p,\kappa_b) \\ &\times K_V^N(r,\ L+1), \end{aligned} \tag{73}$$

where the K_V's are defined in the following way:

$$\begin{aligned} K_V^N(r,\ L) &= \frac{-i}{\sqrt{L(L+1)}}\{j_L(\omega r)(\kappa_p+\kappa_b)[F_1(f_{\kappa_p}g_{\kappa_b} + g_{\kappa_p}f_{\kappa_b}) \\ &+ \frac{F_2\mu_T\omega}{2M}(f_{\kappa_p}g_{\kappa_b} - g_{\kappa_p}f_{\kappa_b})] + \frac{\mu_T\omega}{2M}\frac{F_2}{2L+1}[(\kappa_p+\kappa_b) \\ &\times (f_{\kappa_p}g_{\kappa_b} + g_{\kappa_p}f_{\kappa_b})(Lj_{L+1}(\omega r) - (L+1)j_{L-1}(\omega r)) \\ &+ L(L+1)(f_{\kappa_p}g_{\kappa_b} - g_{\kappa_p}f_{\kappa_b})(j_{L+1}(\omega r) + j_{L-1}(\omega r))]\} \end{aligned} \tag{74}$$

$$\begin{aligned} K_V^N(r,\ L-1) &= \frac{i}{\sqrt{L(2L+1)}}\{j_{L-1}(\omega r)[(F_1(\kappa_p-\kappa_b) - L\frac{F_2\mu_T\omega}{2M}) \\ &\times (f_{\kappa_p}g_{\kappa_b} + g_{\kappa_p}f_{\kappa_b}) + ((\kappa_p-\kappa_b)\frac{F_2\mu_T\omega}{2M} - LF_1)(f_{\kappa_p}g_{\kappa_b} - g_{\kappa_p}f_{\kappa_b})] \\ &+ \frac{F_2\mu_T\omega}{2M}(\kappa_p-\kappa_b)j_L(\omega r)(f_{\kappa_p}f_{\kappa_b} + g_{\kappa_p}g_{\kappa_b})\} \end{aligned} \tag{75}$$

$$K_V^N(r,\ L+1) = \frac{i}{\sqrt{(L+1)(2L+1)}}\{j_{L+1}(\omega r)[(F_1(\kappa_p-\kappa_b) + (L+1)\frac{F_2\mu_T\omega}{2M})(f_{\kappa_p}g_{\kappa_b}+g_{\kappa_p}f_{\kappa_b}) + ((\kappa_p-\kappa_b)\frac{F_2\mu_T\omega}{2M} + (L+1)F_1)(f_{\kappa_p}g_{\kappa_b}-g_{\kappa_p}f_{\kappa_b})] - \frac{F_2\mu_T\omega}{2M}(\kappa_p-\kappa_b)j_L(\omega r) \times (f_{\kappa_p}f_{\kappa_b}+g_{\kappa_p}g_{\kappa_b})\} \quad (76)$$

In the same way, the corresponding integrals for the electron part are given by

$$\int \bar{\psi}_f\hat{j}_0\psi_i j_L(\omega r)Y_L^{M*}(\hat{r})d\Omega = (-1)^M\langle J_i\mu_i, L-M|J_f\mu_f\rangle I_L(\kappa_f,\kappa_i) \times K_S^E(r), \quad (77)$$

and

$$\int \bar{\psi}_f\hat{\mathbf{j}}\psi_i j_L(\omega r)\cdot\mathbf{Y}_{L\ J}^{M\ *}(\hat{r})d\Omega = \langle J_i\mu_i, L-M|J_f\mu_f\rangle I_L(-\kappa_f,\kappa_i) \times (-1)^{L+J+M+1}K_V^E(r,\ J), \quad (78)$$

where J represents L, $L+1$, and $L-1$.

In our analysis we are looking at one particular shell, and trying to find the reduced cross section ρ_m , which for plane waves in the final state is related to the probability that a bound proton from a given shell with the missing momentum p_m can be knocked out of the nucleus with asymptotic momentum $\mathbf{p}$. The reduced cross section as a function of p_m is commonly defined by

$$\rho_m(p_m) = \frac{1}{pE_p\sigma_{ep}}\frac{d^3\sigma}{dE_f d\Omega_f d\Omega_p}, \quad (79)$$

where σ_{ep} denotes the off-shell electron-proton cross section.

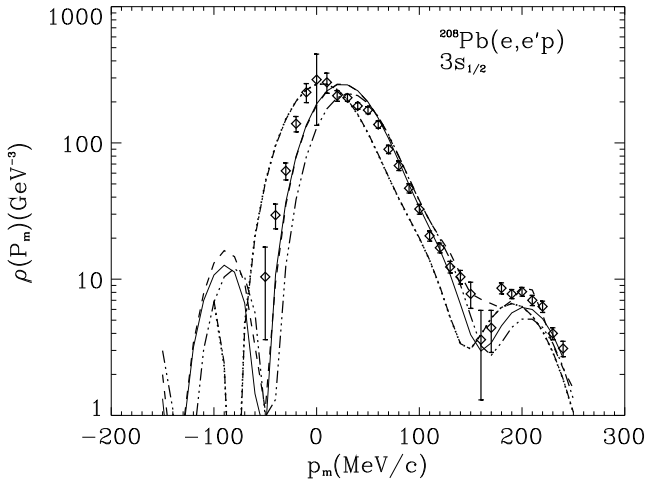

FIG. 5: Reduced cross sections for $^{208}\mathrm{Pb}(e,e'p)$ from the $3s_{1/2}$ shell with parallel kinematics. The kinematics are E=412 MeV, and proton kinetic energy T=100 MeV. The dotted line is the PWBA result and the dash-dotted line, the solid line is the approximate DWBA result, and the diamonds are data from NIKHEF.

3.4 Rosenbluth Separation

In the extreme relativistic limit ($m_e = 0$), the sum over labels of the electron tensor can be explicitly carried out using the spin projection operator for the initial electron and the Trace Theorem:

$$\begin{aligned}\eta^{\mu\nu} &= \sum_{s_i s_f}[\bar{u}(p_f)\gamma^\mu u(p_i)]^*[\bar{u}(p_f)\gamma^\nu u(p_i)] = \frac{1}{8}Tr[\not{p}_f\gamma^\mu(1+h\gamma^5)\not{p}_i\gamma^\nu] \\ &= \frac{1}{2p_ip_f}[p_i^\mu p_f^\nu + p_i^\nu p_f^\mu - g^{\mu\nu}(E_iE_f - \mathbf{p}_i\cdot\mathbf{p}_f) + ih\epsilon^{\mu\nu\delta\lambda}p_{f\delta}p_{i\lambda}] \qquad (80)\end{aligned}$$

where h is $+1$ for positive electron helicity and -1 for negative electron helicity.

The first three terms of the electron tensor in Eq. (80) are symmetric with respect to interchanging μ and ν, and independent of the electron helicity. However, the last term is antisymmetric for μ and ν, and depends on the electron helicity h. Therefore, the electron tensor can be written as the

summation of a symmetric and an antisymmetric tensor:

$$\eta^{\mu\nu} = \eta_S^{\mu\nu} + \eta_A^{\mu\nu}. \tag{81}$$

The general form of a nuclear tensor $W_{\mu\nu}$ can be constructed with the energy momentum four vectors q^μ, p^μ, and p_b^μ using four momentum conservation, and electromagnetic current conservation requires $q^\mu W_{\mu\nu} = q^\nu W_{\nu\mu} = 0$. Thus, the nuclear tensor can be written as

$$\begin{aligned} W_{\mu\nu} &= W_1 g_{\mu\nu} + W_2 p_{b\mu} p_{b\nu} + W_3 p_\mu p_\nu \\ &+ W_4(p_{b\mu} p_\nu + p_{b\nu} p_\mu) + W_5(p_{b\mu} p_\nu - p_{b\nu} p_\mu). \end{aligned} \tag{82}$$

The constraints were satisfied by constructing $W_{\mu\nu}$ from a complete set of four vectors and second rank tensors. Each coefficient W_1–W_5 depends only on Lorentz scalars involving the momentum transfer and the hadron momenta. This nuclear tensor, just as the electron tensor, consists of a symmetric and an antisymmetric part in the labels μ ν. The first four terms of the nuclear tensor are symmetric and the last term is antisymmetric under interchanging μ and ν:

$$W_{\mu\nu} = W_{\mu\nu}^S + W_{\mu\nu}^A. \tag{83}$$

Since the contraction of a symmetric and an antisymmetric tensor yields zero, the contraction of the electron and nuclear tensor can be written as

$$\eta^{\mu\nu} W_{\mu\nu} = \eta_S^{\mu\nu} W_{\mu\nu}^S + \eta_A^{\mu\nu} W_{\mu\nu}^A. \tag{84}$$

By using the contraction of electron and nuclear tensors, the cross section for electron scattering from a unpolarized target is given by

$$\frac{d^3\sigma}{dE_f d\Omega_f d\Omega_p} = \frac{1}{2}\frac{2\pi}{I_{in}} \rho_e \rho_p \frac{1}{2j_b+1} \frac{(4\pi\alpha)^2}{q_\mu^4} (\eta_s^{\mu\nu} W_{\mu\nu}^S + \eta_A^{\mu\nu} W_{\mu\nu}^A)$$

$$= \frac{pE_p}{(2\pi)^3}\sigma_M[\frac{q_\mu^4}{q^4}R_L + (\tan^2\frac{\theta_e}{2} - \frac{q_\mu^2}{2q^2})R_T - \frac{q_\mu^2}{2q^2}\cos 2\phi_p R_{TT}$$
$$- \frac{q_\mu^2}{q^2}(\tan^2\frac{\theta_e}{2} - \frac{q_\mu^2}{q^2})^{1/2}\cos\phi_p R_{LT} - h\frac{q_\mu^2}{q^2}\tan\frac{\theta_e}{2}\sin\phi_p R_{LT'}], \quad (85)$$

where

$$R_L(q,\omega) = \frac{q^4}{q_\mu^4}W_{00}, \quad R_T(q,\omega) = W_{11} + W_{22}$$
$$\cos 2\phi_P R_{TT}(q,\omega) = W_{11} - W_{22}, \quad \cos\phi_P R_{LT}(q,\omega) = -\frac{q^2}{q_\mu^2}(W_{01} + W_{10})$$
$$\sin\phi_P R_{LT'}(q,\omega) = -i\frac{q^2}{q_\mu^2}(W_{02} + W_{20}).$$

σ_M denotes the Mott cross section given by $\sigma_M = (\frac{\alpha}{2E})^2\frac{\cos^2\frac{\theta_e}{2}}{\sin^4\frac{\theta_e}{2}}$.

The reduced cross section ρ_m is introduced, which is related to the probability that a bound nucleon from a given orbit with the missing momentum p_m can be knocked out of the nucleus with asymptotic momentum p. The reduced cross section as a function of p_m is commonly defined by

$$\rho_m(p_m) = \frac{1}{pE_p\sigma_{ep}}\frac{d^3\sigma}{dE_f d\Omega_f d\Omega_p}, \quad (86)$$

where the missing momentum is determined by the kinematics, $\mathbf{p}_m = \mathbf{p} - \mathbf{q}$. The off-shell electron-proton cross section, σ_{ep}, is not uniquely defined but we use the form σ_{ep}^{cc1}.

There are two kinds of experimental kinematics, parallel and perpendicular kinematics. In the perpendicular kinematics, the polar angle of the knocked-out proton is measured with respect of the momentum transfer where the magnitude of $\mathbf{p}$ is fixed at $|\mathbf{p}| = |\mathbf{q}|$, and in the parallel kinematics, the magnitude of the missing momentum $\mathbf{p}_m$ changes at which $\mathbf{p}$ is parallel to $\mathbf{q}$. In the parallel kinematics, the three interference terms in Eq. (85) disappear

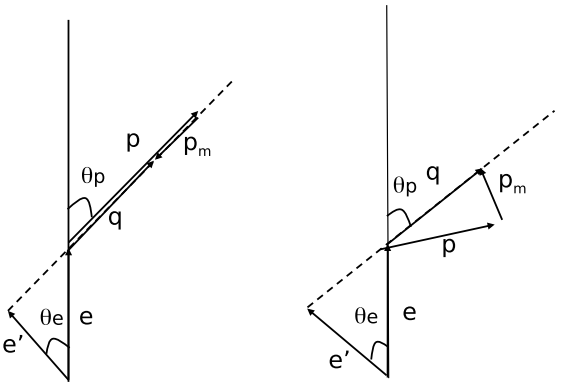

FIG. 6: The left panel is the parallel kinematics and the right is the perpendicular kinematics.

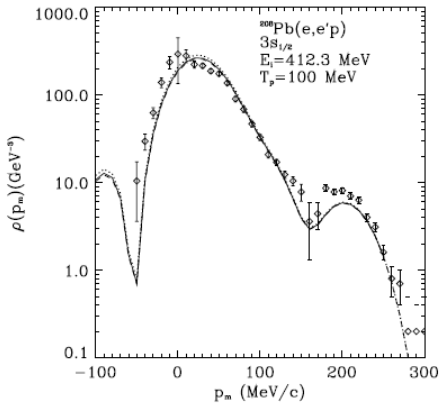

FIG. 7: The cross sections in parallel kinematics from the $3s_{1/2}$ orbit of ^{208}Pb target as a function of the missing momentum. The incident electron energy is 412 MeV, the proton kinetic energy is 100 MeV, and the data are from NIKHEF.

due to integrating over the azimuthal angle ϕ_p, while all terms remain in the perpendicular kinematics except the fifth term which sums to zero for unpolarized incident electron beam.

3.5 Response Function and Asymmetry

The cross section is given by

$$\begin{aligned}\frac{d^3\sigma}{dE_f d\Omega_f d\Omega_p} &= \frac{pE_p}{(2\pi)^3}\sigma_M[v_L R_L + v_T R_T - v_{TT}\cos 2\phi_p R_{TT} \\ &- v_{LT}\cos\phi_p R_{LT} - h v_{LT'}\sin\phi_p R_{LT'}].\end{aligned}$$

The fourth response function could be obtained by subtracting the cross sections at azimuthal angles of the outgoing proton $\phi_p = 0$ and $\phi_p = \pi$ and

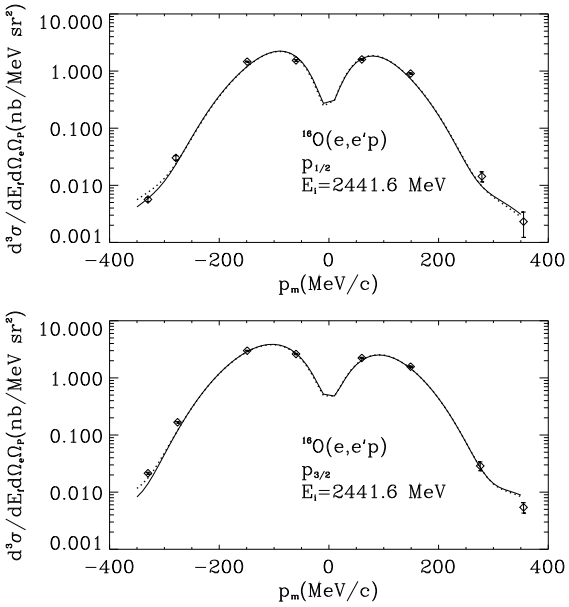

FIG. 8: The cross sections in perpendicular kinematics from the $p_{1/2}$ and $p_{3/2}$ orbits of ^{16}O targets as a function of the missing momentum. The incident electron energy is 2441.6 MeV, the proton kinetic energy is 427 MeV, and the data are from Jlab.

keeping the other electron and outgoing proton kinematics variables fixed. The fourth response function is a function of the missing momentum given by

$$R_{LT} = \frac{\sigma^R - \sigma^L}{2K v_{LT}} \ , \tag{87}$$

where L (left) and R (right) indicate the left side at $\phi_p = 0$ and the right side at $\phi_p = \pi$ of the cross section, respectively. The kinematics factor K is $K = (pE_p\sigma_M)/(2\pi^3)$. Of course, this fourth response function can be directly calculated in the PWBA.

If the incident electron beam is polarized, helicity h=1, one can obtain the fifth response function by subtracting the down part ($-\pi < \phi_p < 0$) from the up part ($0 < \phi_p < \pi$) of the cross section with respect to the scattering plane, while all other kinematics variables are kept the same. The fifth structure

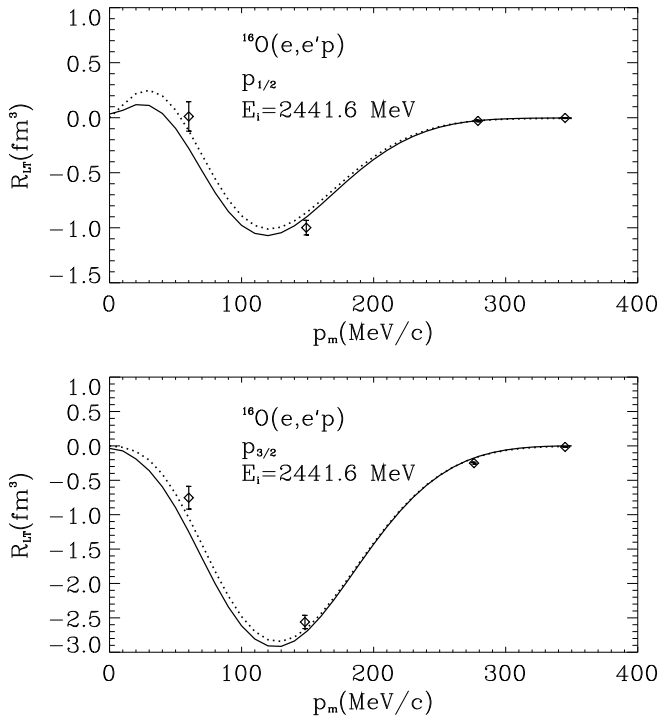

FIG. 9: The fourth response functions from the $p_{1/2}$ and $p_{3/2}$ orbits of ^{16}O as a function of the missing momentum. The solid lines are the extracted fourth functions for the DWBA results, the dotted lines are the PWBA results, and the diamonds are data from Jlab.

function can be written as

$$R_{LT'} = \frac{\sigma^U - \sigma^D}{2Kv_{LT'}\sin\phi_p} \ , \tag{88}$$

where U and D indicate the "up" and "down" part of the cross section, respectively. This clearly describes the "up-down" asymmetry of the cross section with respect to the scattering plane.

We also calculate another left-right asymmetry, A_{LT}, defined as

$$A_{LT} = \frac{\sigma^R - \sigma^L}{\sigma^R + \sigma^L} \ . \tag{89}$$

In this case, the kinematics is the same as for the fourth structure function in eq. (87).

On the other hand, by adding the left side and the right side of the cross

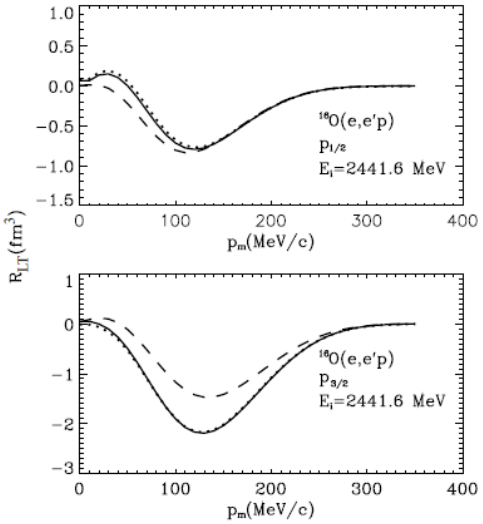

FIG. 10: The fifth response functions from the $p_{1/2}$ and $p_{3/2}$ orbits of ^{16}O as a function of the missing momentum. The azimuthal angle of knocked-out proton is $\phi_p = 40^0$

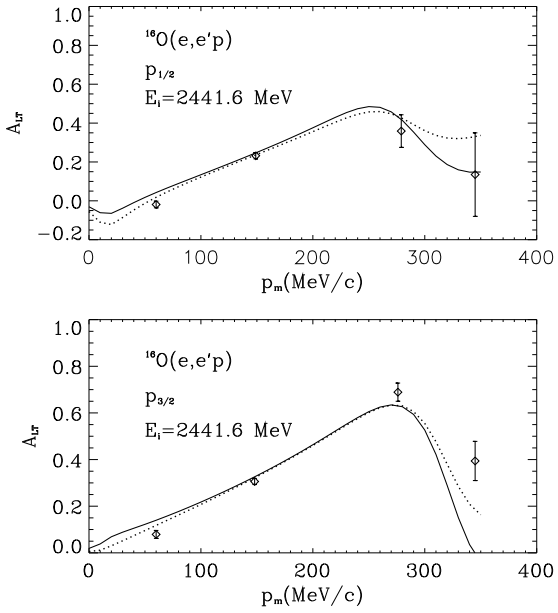

FIG. 11: The asymmetry for the ^{16}O target.

section, one can obtain the second response function as

$$\frac{\sigma^L + \sigma^R}{2K} = R_T + x(\theta)(R_L + \frac{v_{TT}}{v_L} R_{TT}), \tag{90}$$

where $x(\theta) = \frac{v_L}{v_T}$ is a function of the electron scattering angle θ.

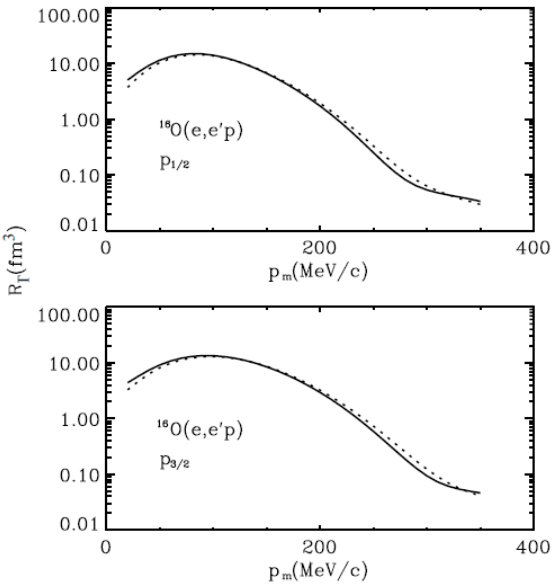

FIG. 12: The transverse response functions from the $p_{1/2}$ and $p_{3/2}$ orbits of ^{16}O as a function of the missing momentum.

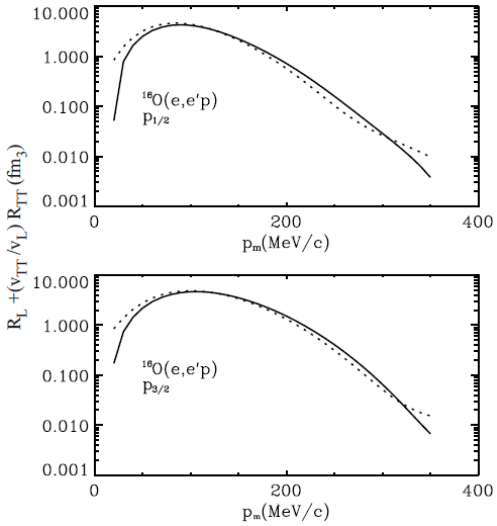

FIG. 13: The $R_L + \frac{v_{TT}}{v_L} R_{TT}$ response functions from the $p_{1/2}$ and $p_{3/2}$ orbits of ^{16}O as a function of the missing momentum.

3.6 Inclusive (e, e') reaction

The cross section for the $(e, e'p)$ reaction is written as

$$\frac{d^3\sigma}{dE_f d\Omega_f d\Omega_p} = \frac{pE_p}{(2\pi)^3}\sigma_M[v_L R_L + v_T R_T - v_{TT}\cos 2\phi_p R_{TT} - v_{LT}\cos\phi_p R_{LT} - h v_{LT'}\sin\phi_p R_{LT'}].$$

In inclusive processes, the ejected nucleons are not observed, whereas they are observed in the exclusive processes. The cross section in the (e, e') reaction can be calculated by integrating over the ejected nucleon angle $d\Omega_p$ and summing over all the possible channels for the excited nuclear system. We consider the PWBA calculation with the partial wave expansion. The explicit form for the nuclear form factors N_0 and $\mathbf{N}_T$ in the PWBA are defined as the Fourier transforms of the nuclear transition current;

$$N_0 = \int J_0(\mathbf{r}) e^{i\mathbf{q}\cdot\mathbf{r}} d^3r \tag{91}$$

$$\begin{aligned} \mathbf{N}_T &= \int \mathbf{J_T}(\mathbf{r}) e^{i\mathbf{q}\cdot\mathbf{r}} d^3r \\ &= \sum_{\lambda=\pm1} \hat{\xi}^*_\lambda \int \mathbf{J}(\mathbf{r})\cdot\hat{\xi}_\lambda e^{i\mathbf{q}\cdot\mathbf{r}} d^3r \end{aligned} \tag{92}$$

where $\mathbf{q}$ is an asymptotic momentum transfer along the $\hat{z}$-direction and $\mathbf{J}_T = J_+\hat{\xi}^*_+ + J_-\hat{\xi}^*_-$ in the spherical coordinate, which is given by $\hat{\xi}_0 = \hat{z}$, $\hat{\xi}_{\pm1} = \mp\frac{1}{\sqrt{2}}(\hat{x} \pm i\hat{y})$. By using the partial wave expansion, we can easily get the longitudinal term in the form;

$$\begin{aligned} N_0 = \sqrt{4\pi} \sum_{\kappa_p\mu_p m_p} \sum_{LM} & \sqrt{2L+1} \langle l_p m_p, \frac{1}{2} s_p | j_p \mu_p \rangle Y^{m_p *}_{l_p}(\hat{p}) e^{-i\delta^*_{\kappa_p}} \\ & \langle j_b \mu_b, LM | j_p \mu_p \rangle R_{\kappa_p \kappa_b}(q; L). \end{aligned} \tag{93}$$

The transverse term can be written in spherical coordinates

$$\mathbf{N}_T = N_+\hat{\xi}^*_+ + N_-\hat{\xi}^*_- \tag{94}$$

where

$$\begin{aligned} N_+ = \sqrt{2\pi} \sum_{\kappa_p\mu_p m_p} \sum_{LM} & \sqrt{2L+1} \langle l_p m_p, \frac{1}{2} s_p | j_p \mu_p \rangle Y^{m_p *}_{l_p}(\hat{P}) e^{-i\delta^*_{\kappa_p}} \\ & \langle j_b \mu_b, LM | j_p \mu_p \rangle [R_{\kappa_p \kappa_b}(q; M) + R_{\kappa_p \kappa_b}(q; E)] \end{aligned} \tag{95}$$

$$N_- = -\sqrt{2\pi}\sum_{\kappa_p\mu_p m_p}\sum_{LM}\sqrt{2L+1}\langle l_p m_p, \frac{1}{2}s_p|j_p\mu_p\rangle Y_{l_p}^{m_p *}(\hat{p})e^{-i\delta^*_{\kappa_p}}$$
$$\langle j_b\mu_b, LM|j_p\mu_p\rangle[R_{\kappa_p\kappa_b}(q;M) - R_{\kappa_p\kappa_b}(q;E)]. \quad (96)$$

The label L, M and E denote the longitudinal, magnetic and electric terms. By using the Dirac multipole operator matrix element given in the Appendix, we have each term explicitly;

$$R_{\kappa_{pp}\kappa_b}(q;L) = (4\pi)\sqrt{\frac{E_p+M}{2E_p}}\sqrt{\frac{E_b+M}{2E_b}}(i)^{l_p+L}I_L(\kappa_p,\kappa_b)$$
$$\int drr^2\{F_1(f^*_{\kappa_p}f_{\kappa_b}+g^*_{\kappa_p}g_{\kappa_b})j_L(qr) + \frac{\mu_T F_2 q}{2M(2L+1)}$$
$$[(-Lj_{L-1}(qr)+(L+1)j_{L+1}(qr))(f^*_{\kappa_p}g_{\kappa_b}+g^*_{\kappa_p}f_{\kappa_b})$$
$$+(\kappa_p-\kappa_b)(j_{L-1}(qr)+j_{L+1}(qr))(f^*_{\kappa_p}g_{\kappa_b}-g^*_{\kappa_p}f_{\kappa_b})]\} \quad (97)$$

$$R_{\kappa_p\kappa_b}(q;M) = (4\pi)\sqrt{\frac{E_p+M}{2E_p}}\sqrt{\frac{E_b+M}{2E_b}}\frac{(i)^{l_p+L+1}}{\sqrt{L(L+1)}}I_L(\kappa_p,-\kappa_b)$$
$$\int drr^2\{F_1(\kappa_p+\kappa_b)(f^*_{\kappa_p}g_{\kappa_b}+g^*_{\kappa_p}f_{\kappa_b})j_L(qr)$$
$$+\frac{\mu_T F_2\omega}{2M}(\kappa_p+\kappa_b)(f^*_{\kappa_p}g_{\kappa_b}-g^*_{\kappa_p}f_{\kappa_b})j_L(qr)$$
$$+\frac{\mu_T F_2\omega}{2M(2L+1)}[L(L+1)(f^*_{\kappa_p}f_{\kappa_b}-g^*_{\kappa_p}g_{\kappa_b})$$
$$(j_{L-1}(qr)+j_{L+1}(qr))+(\kappa_p+\kappa_b)$$
$$(Lj_{L+1}(qr)-(L+1)j_{L-1}(qr))(f^*_{\kappa_p}f_{\kappa_b}+g^*_{\kappa_p}g_{\kappa_b})]\} \quad (98)$$

$$R_{\kappa_p\kappa_b}(q;E) = (4\pi)\sqrt{\frac{E_p+M}{2E_p}}\sqrt{\frac{E_b+M}{2E_b}}\frac{(i)^{l_p+L}I_L(\kappa_p,\kappa_b)}{(2L+1)\sqrt{L(L+1)}}$$
$$\int drr^2\{F_1[(\kappa_p-\kappa_b)(f^*_{\kappa_p}g_{\kappa_b}+g^*_{\kappa_p}f_{\kappa_b})(Lj_{L+1}(qr)-(L+1)$$
$$j_{L-1}(qr))+L(L+1)(f^*_{\kappa_p}g_{\kappa_b}-g^*_{\kappa_P}f_{\kappa_b})(j_{L-1}(qr)+j_{L+1}(qr))]$$

$$+\frac{\mu_T F_2 \omega}{2M}[L(L+1)(f^*_{\kappa_p} g_{\kappa_b} + g^*_{\kappa_p} f_{\kappa_b})(j_{L-1}(qr) + j_{L+1}(qr))$$
$$+(\kappa_p - \kappa_b)(f^*_{\kappa_p} g_{\kappa_b} + g^*_{\kappa_p} f_{\kappa_b})(L j_{+-1}(qr) - (L+1) j_{L-1}(qr))]$$
$$-\frac{\mu_T F_2 q}{2M}(2L+1)(\kappa_p - \kappa_b) j_L(qr)(f^*_{\kappa_p} f_{\kappa_b} + g^*_{\kappa_p} g_{\kappa_b})\}. \qquad (99)$$

In the (e, e') process, the longitudinal and the transverse structure functions remain after integrating the cross section in Eq. (85) over the solid angle $d\Omega_P$ of the ejected nucleon. We sum over all quantum numbers and use the following orthogonalities;

$$\int d\Omega_p Y^{m_p *}_{l_p}(\hat{p}) Y^{m'_p}_{l'_p}(\hat{p}) = \delta_{l_p l'_p} \delta_{m_p m'_p}$$
$$\sum_{m_p s_p} \langle l_p m_p, \frac{1}{2} s_p | j_p \mu_p \rangle \langle l_p m_p, \frac{1}{2} s_p | j'_p \mu'_p \rangle = \delta_{j_p j'_p} \delta_{\mu_p \mu'_p}$$
$$\sum_{\mu_p \mu_b} \langle j_b \mu_b, LM | j_p \mu_p \rangle \langle j_b \mu_b, L'M' | j_p \mu_p \rangle = \frac{2j_p + 1}{2L+1} \delta_{LL'} \delta_{MM'}.$$

Finally, the longitudinal and the transverse structure functions become

$$R^{in}_L = \int \rho_p R_L d\Omega_p = \frac{\rho_p}{2(2j_b+1)} \sum_{\mu_b s_p} \int |N_0|^2 d\Omega_p$$
$$= \frac{4\pi \rho_p}{2(2j_b+1)} \sum_{\kappa_P LM} (2j_p + 1) e^{2Im(\delta_{\kappa_p})} |R_{\kappa_p \kappa_b}(q; L)|^2 \qquad (100)$$

$$R^{in}_T = \int \rho_p R_T d\Omega_p = \frac{\rho_p}{2(2j_b+1)} \sum_{\mu_b s_p} \int (|N_+|^2 + |N_-|^2) d\Omega_p$$
$$= \frac{4\pi \rho_p}{2(2j_b+1)} \sum_{\kappa_p LM} (2j_p + 1) e^{2Im(\delta_{\kappa_p})} (|R_{\kappa_P \kappa_b}(q; M)|^2$$
$$+ |R_{\kappa_p \kappa_b}(q; E)|^2) \qquad (101)$$

where $Im(\delta_{\kappa_P})$ is the imaginary part of the phase shift for the ejected nucleons. In terms of the structure functions, the cross section in (e, e') reaction

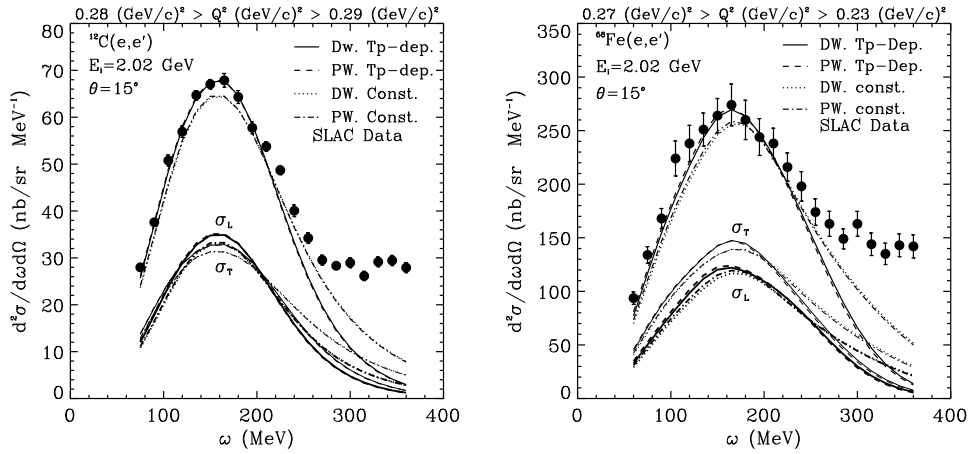

FIG. 14: The comparison with Slac data for ^{12}C, ^{56}Fe.

is given by

$$\frac{d^2\sigma}{dE_f d\Omega_f} = \sigma_M[\frac{q_\mu^4}{q^4}R_L^{in}(q,\omega) + (\tan^2\frac{\theta_e}{2} - \frac{q_\mu^2}{2q^2})R_T^{in}(q,\omega)] \tag{102}$$

where q_μ is the four momentum transfer and σ_M is the Mott cross section. The structure functions depend only on the momentum transfer and the energy transfer.

3.7 Coulomb sum rule

From the measured cross section in Eq. (102), the total structure function is defined as

$$S_{tot}(q,\omega,\theta) = \left(\frac{\epsilon(\theta)}{\sigma_M}\right)\left(\frac{q^4}{Q^4}\right)\frac{d^2\sigma}{d\Omega_f d\omega}, \tag{103}$$

where the $\epsilon(\theta)$ is the virtual photon polarization given by $(1 + \frac{2q^2}{Q^2}\tan^2\frac{\theta_e}{2})^{-1}$ and the four momentum transfer squared is $Q^2 = \omega^2 - q^2 = -q_\mu^2$.

Therefore, the total structure function in Eq. (103) becomes

$$S_{tot}(q,\omega,\theta) = \epsilon(\theta)R_L^{in}(q,\omega) + \left(\frac{q^2}{2Q^2}\right)R_T^{in}(q,\omega). \tag{104}$$

S_{tot} is described as a straight line in terms of the independent variable $\epsilon(\theta)$ with slope $R_L(q,\omega)$ and intercept proportional to $R_T(q,\omega)$ by keeping the momentum transfer q and the energy transfer ω fixed.

The Coulomb sum rule (CSR) is defined as the integration of the total longitudinal structure function in Eq. (104) for inclusive (e,e') reaction

$$C(q) = \frac{1}{Z}\int_{\omega_{min}}^{\infty} \frac{R_L^{in}(q,\omega)}{\tilde{G}_E^2(Q^2)} d\omega, \tag{105}$$

with the electric form factor given by

$$\tilde{G}_E^2(Q^2) = \left[G_{Ep}^2(Q^2) + \frac{N}{Z} G_{En}^2(Q^2)\right] \frac{(1+\tau)}{(1+2\tau)}, \tag{106}$$

where Z and N are number of protons and neutrons of the target, respectively. The last factor corresponds to the relativistic correction factor, in which τ is given by $\tau = Q^2/4M_N^2$ with the nucleon mass M_N.

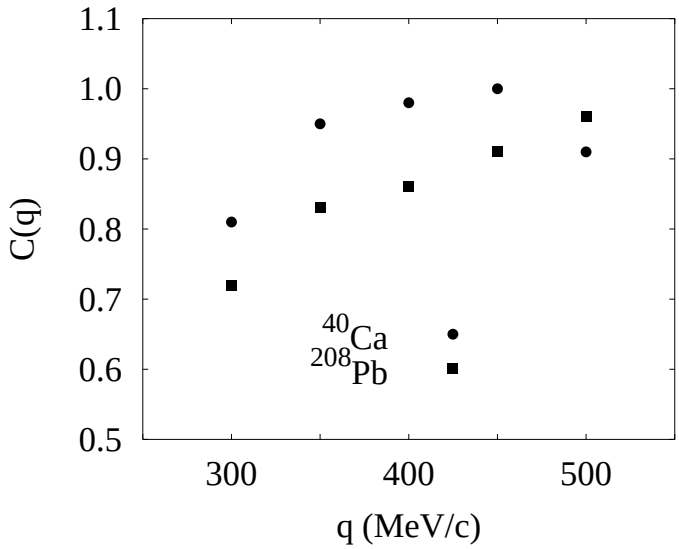

FIG. 15: The Coulomb sum rule for our model in terms of q values. The solid circles are for ^{40}Ca and the solid rectangles are for ^{208}Pb, respectively.

3.8 y-scaling

The cross section for the inclusive (e, e') is written as

$$\frac{d^2\sigma}{d\omega d\Omega_e} = \sigma_M \left\{ \frac{q_\mu^4}{q^4} S_L(q,\omega) + (\tan^2\frac{\theta_e}{2} - \frac{q_\mu^2}{2q^2}) S_T(q,\omega) \right\}, \tag{107}$$

where $\sigma_M = (\alpha/2E)^2[\cos^2(\theta/2)/\sin^4(\theta/2)]$ is the Mott cross section.

The *y*-scaling function is defined as the ratio of measured cross section to off-shell electron-nucleon cross section as following:

$$F(y) = \frac{d^2\sigma}{d\omega d\Omega_e}(Z\sigma_{ep} + N\sigma_{en})^{-1} \frac{q}{[M^2 + (y+q)^2]^{1/2}}, \tag{108}$$

where σ_{ep} (σ_{en}) denotes the off-shell electron-proton(neutron) cross section. Z and N are the number of protons and neutrons, and M is the mass of nucleon. The scaling variable y is given by

$$\omega + M_A = (M^2 + q^2 + y^2 + 2yq)^{1/2} + ({M_{A-1}}^2 + y^2)^{1/2}, \tag{109}$$

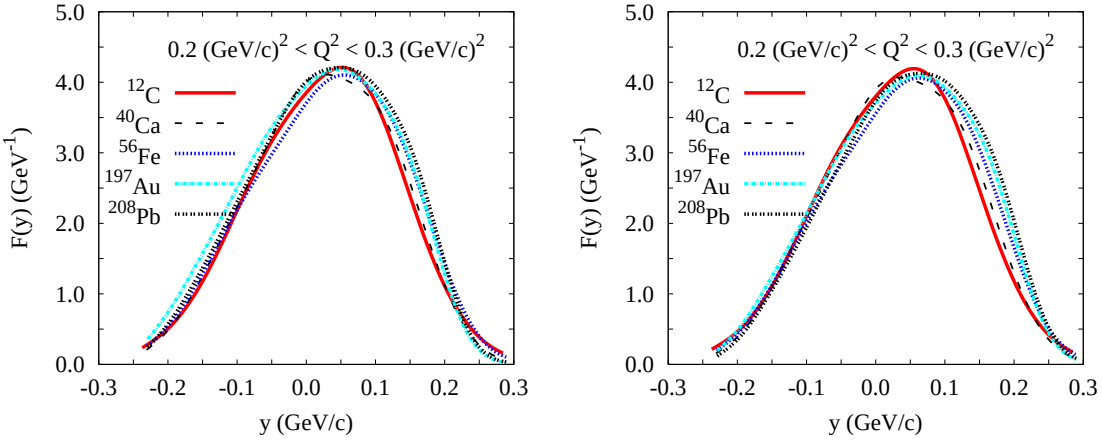

FIG. 16: The y-scaling functions are from ^{12}C, ^{40}Ca, ^{56}Fe, ^{197}Au, and ^{208}Pb with 750 MeV and 45^o. The calculations of the left panel do not include the final state interaction of the outgoing nucleons and electron Coulomb distortion. In the right panel, the final state interaction is not included but electron Coulomb distortion is included.

where M_A is the mass of the target nucleus and M_{A-1} is the mass of the ground state of the $A-1$ nucleus. The point $y=0$ corresponds to the peak of the quasielastic scattering and $y<0$ ($y>0$) corresponds to the small (large) ω region.

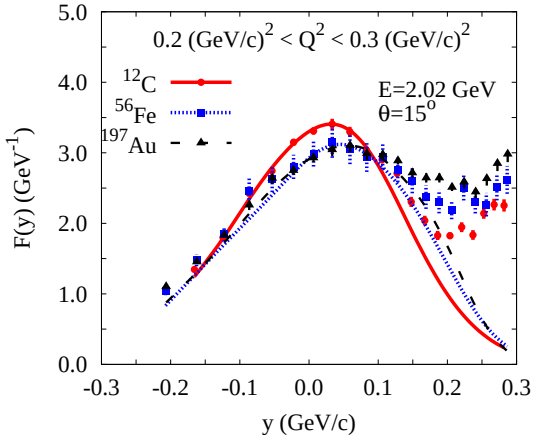

FIG. 17: The y-scaling functions for three different target nuclei from ^{12}C (dash-dot and ▲), ^{56}Fe (solid and •), and ^{197}Au (dot and ■). The electron energy is $E = 2.02$ GeV and the scattering angle is $\theta = 15^o$. The experimental data are from SLAC.

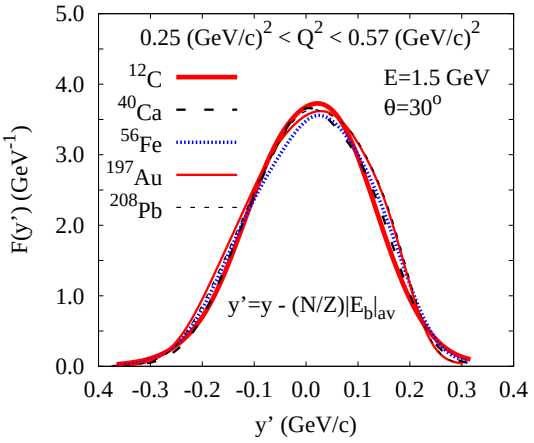

FIG. 18: The new y'-scaling functions are for the high electron energy $E = 1.5$ GeV and the scattering angle $\theta = 30^o$ from several nuclei.

3.9 Parity violation

Our formalism is based on the Born approximation with single photon and Z^0 boson exchange by the standard electro-weak theory. In the laboratory frame, the inclusive cross section, which does not detect the outgoing nucleons, is given by the contraction between lepton and hadron tensor. Since the

kinematic factor of polarized scattering cross sections are canceled each other, the asymmetry of the parity violation(PV) electron scattering is written as follows:

$$A = \frac{\frac{d\sigma^+}{d\Omega_f dE_f} - \frac{d\sigma^-}{d\Omega_f dE_f}}{\frac{d\sigma^+}{d\Omega_f dE_f} + \frac{d\sigma^-}{d\Omega dE_f}} = A_0 \frac{W_{PV}}{W_{EM}}, \tag{110}$$

where the constant A_0 is given by

$$A_0 = \frac{G_F Q^2}{2\pi\alpha\sqrt{2}}, \tag{111}$$

with the Fermi constant G_F and the fine structure constant α.

The electromagnetic total response function is decomposed into the longitudinal and transverse response functions as follows:

$$W_{EM} = v_L R^L_{EM} + v_T R^T_{EM}, \tag{112}$$

where $R^L_{EM} = |J^0_{EM}|^2$ is the longitudinal response function and $R^T_{EM} = |J^x_{EM}|^2 + |J^y_{EM}|^2$ is the transverse response function. The weak current is the summation of neutral vector current and neutral axial vector current through Z^0 boson exchange:

$$W_{PV} = W^V_{PV} + W^A_{PV}. \tag{113}$$

The weak vector current is given by

$$W^V_{PV} = v_L R^L_{PV} + v_T R^T_{PV}, \tag{114}$$

where the longitudinal and transverse response functions are given by $R^L_{PV} = J^{0*}_{EM} J^0_{NC}$ and $R^T_{PV} = J^{x*}_{EM} J^x_{NC} + J^{y*}_{EM} J^y_{NC}$, respectively. The weak axial vector current is written as

$$W^A_{PV} = v'_T R^{T'}_{PV}, \tag{115}$$

where the transverse response function is contributed in the way $R_{PV}^{T'} = J_{EM}^{*} J_{AV}^{NC}$. The factors of the electron kinematics are given by

$$v_L = \frac{Q^4}{q^4}, \quad v_T = \tan^2\frac{\theta_e}{2} + \frac{Q^2}{2q^2}, \quad \text{and} \quad v'_T = \tan\frac{\theta_e}{2}\sqrt{\tan^2\frac{\theta_e}{2} + \frac{Q^2}{q^2}}, \tag{116}$$

where θ_e denotes the scattering angle.

The nuclear current is calculated by the Fourier transform of nucleon current operator:

$$J^\mu = \int \bar{\psi}_p \hat{\mathbf{J}}^\mu \psi_b e^{i\mathbf{q}\cdot\mathbf{r}} d^3r, \tag{117}$$

where $\hat{\mathbf{J}}^\mu$ is a free weak nucleon current operator. For a free nucleon, the current operator for the electromagnetic interaction is composed of the Dirac and the Pauli form factors given by

$$\hat{\mathbf{J}}^\mu_{EM} = F_1(Q^2)\gamma^\mu + F_2(Q^2)\frac{i\kappa}{2M_N}\sigma^{\mu\nu}q_\nu, \tag{118}$$

where κ represents nucleon magnetic moment.

The current operator of the neutral current reaction consists of the weak vector and the axial vector form factors given by

$$\hat{\mathbf{J}}^\mu_{NC} = F_1^V(Q^2)\gamma^\mu + F_2^V(Q^2)\frac{i\kappa}{2M_N}\sigma^{\mu\nu}q_\nu. \tag{119}$$

By the conservation of the vector current (CVC) hypothesis, the vector form factors for the proton (neutron), $F_i^{V,\ p(n)}(Q^2)$, are expressed as

$$F_i^{V,\ p(n)}(Q^2) = \left(\frac{1}{2} - 2\sin^2\theta_W\right) F_i^{p(n)}(Q^2) - \frac{1}{2}F_i^{n(p)}(Q^2) - \frac{1}{2}F_i^s(Q^2), \tag{120}$$

where θ_W is the Weinberg angle given by $\sin^2\theta_W = 0.2224$.

The strange vector form factors are usually given by a dipole form, independently of the nucleon isospin,

$$F_1^s(Q^2) = \frac{F_1^s(0)Q^2}{(1+\tau)(1+Q^2/M_V^2)^2}\ ,$$

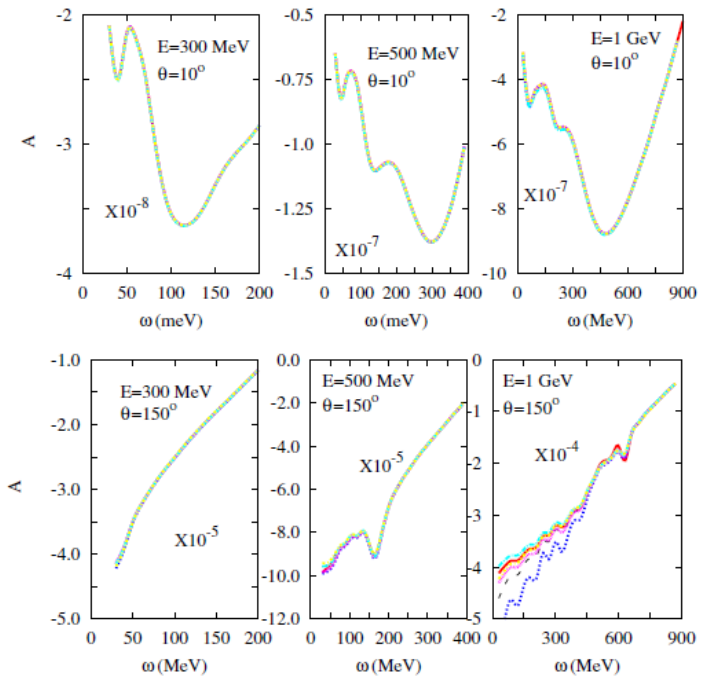

FIG. 19: (Color online) The asymmetry of the parity violation from ^{208}Pb.

$$F_2^s(Q^2) = \frac{F_2^s(0)}{(1+\tau)(1+Q^2/M_V^2)^2} \ , \tag{121}$$

where $\tau = Q^2/(4M_N^2)$ and $M_V = 0.843$ GeV is the cut off mass parameter usually adopted for nucleon electromagnetic form factors. $F_1^s(0)$ is defined as the squared strange radius of the nucleus, $F_1^s(0) = -<r^2>/6 = dG_E^s(Q^2)/dQ^2|_{Q^2=0} = 0.53$ GeV^{-2}, and $F_2^s(0) = \mu_s = -0.04$ is an anomalous strange magnetic moment.

The axial vector current operator is given by

$$\hat{\mathbf{J}}^{\mu}_{AV} = G_A(Q^2)\gamma^{\mu}\gamma^5. \tag{122}$$

The axial form factors for the neutral current reaction are given by

$$G_A(Q^2) = \frac{1}{2}(\mp g_A + g_A^s)/(1+Q^2/M_A^2)^2, \tag{123}$$

where $g_A = 1.262$, $M_A = 1.032$ GeV, and $g_A^s = -0.19$, which represent

the strange quark contents on the nucleon. $-(+)$ coming from the isospin dependence denotes the knocked-out proton (neutron), respectively.

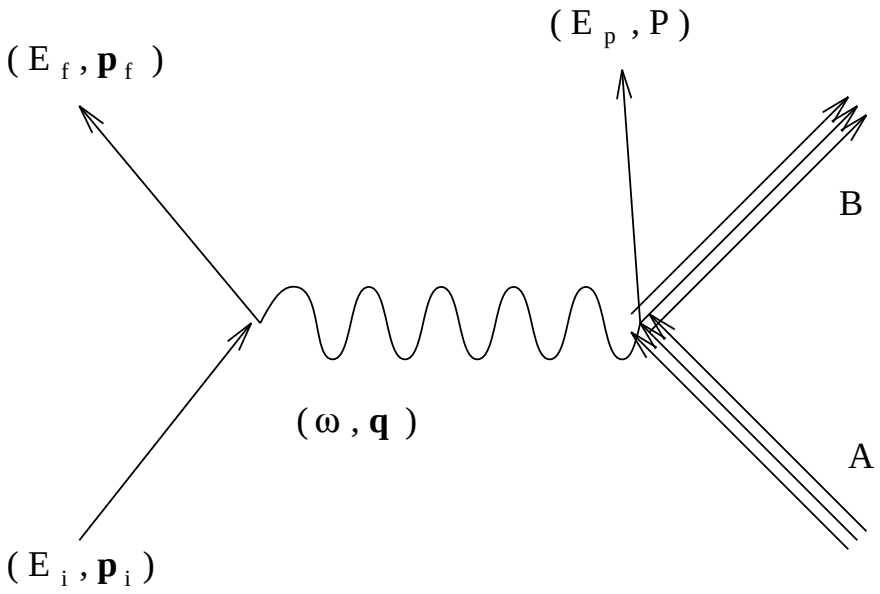

IV. The neutrino-nucleus scattering

We start from a weak current on the nucleon level. The weak current, J^μ, which takes a $V^\mu - A^\mu$ current form by the standard electro-weak theory, represents the Fourier transform of the nucleon current density written as

$$J^\mu = \int \bar{\psi}_p \hat{\mathbf{J}}^\mu \psi_b e^{i\mathbf{q}\cdot\mathbf{r}} d^3r, \tag{124}$$

where $\hat{\mathbf{J}}^\mu$ is a free weak nucleon current operator, and ψ_p and ψ_b are wave functions of the knocked-out and the bound state nucleon, respectively. For a free nucleon, the current operator comprises the weak vector and the axial vector form factors

$$\hat{\mathbf{J}}^\mu = F_1^V(Q^2)\gamma^\mu + F_2^V(Q^2)\frac{i}{2M_N}\sigma^{\mu\nu}q_\nu + G_A(Q^2)\gamma^\mu\gamma^5 + \frac{1}{2M_N}G_P(Q^2)q^\mu\gamma^5, \tag{125}$$

where M_N denotes the mass of the nucleon. By the conservation of the vector current (CVC) hypothesis, vector form factors for the proton (neutron),

$F_i^{V,\ p(n)}(Q^2)$, is expressed as

$$F_i^{V,\ p(n)}(Q^2) = \left(\frac{1}{2} - 2\sin^2\theta_W\right) F_i^{p(n)}(Q^2) - \frac{1}{2}F_i^{n(p)}(Q^2) - \frac{1}{2}F_i^s(Q^2), \quad \text{for the NC}$$
$$F_i^V(Q^2) = F_i^p(Q^2) - F_i^n(Q^2), \quad \text{for the CC} \qquad (126)$$

where θ_W is the Weinberg angle given by $\sin^2\theta_W = 0.2224$.

The neutral current (NC) reaction is $\nu(\bar{\nu}) + N \to \nu'(\bar{\nu}') + N$.

The charged current (CC) reaction is $\nu_\mu(\bar{\nu}_\mu) + p(n) \to \mu^-(\mu^+) + n(n)$.

The strange vector form factors are usually given as a dipole form, independently of the nucleon isospin,

$$F_1^s(Q^2) = \frac{F_1^s Q^2}{(1+\tau)(1+Q^2/M_V^2)^2},$$
$$F_2^s(Q^2) = \frac{F_2^s(0)}{(1+\tau)(1+Q^2/M_V^2)^2}, \qquad (127)$$

where $\tau = Q^2/(4M_N^2)$ and $M_V = 0.843$ GeV is the cut off mass parameter usually adopted for nucleon electromagnetic form factors. F_1^s is defined as the squared strange radius of the nucleus, $F_1^s = -\ <r^2>\ /6 = dG_E^s(Q^2)/dQ^2|_{Q^2=0} = 0.53\ \text{GeV}^{-2}$, and $F_2^s(0) = \mu_s$ is an anomalous strange magnetic moment.

The axial form factors are given by

$$G_A(Q^2) = \frac{1}{2}(\mp g_A + g_A^s)/(1+Q^2/M_A^2)^2, \quad \text{for the NC}$$
$$G_A(Q^2) = -g_A/(1+Q^2/M_A^2)^2, \quad \text{for the CC} \qquad (128)$$

where $g_A = 1.262$, $M_A = 1.032$ GeV, and $g_A^s = -0.19$, which represents the strange quark contents on the nucleon. $-(+)$ coming from the isospin dependence denotes the knocked-out proton (neutron), respectively. The g_A^s represents the strange quark contents in the nucleon.

The induced pseudoscalar form factor is parameterized by the Goldberger-Treimann relation

$$G_P(Q^2) = \frac{2M_N}{Q^2 + m_\pi^2} G_A(Q^2), \tag{129}$$

where m_π is the pion mass. But the contribution of the pseudoscalar form factor vanishes for the NC reaction because of the negligible final lepton mass participating in this reaction.

In the laboratory frame, the inclusive cross section, which does not detect the outgoing ν ($\bar{\nu}$), is given by the contraction between lepton and hadron tensor

$$\begin{aligned} \frac{d\sigma}{dT_p} &= 4\pi^2 \frac{M_N M_{A-1}}{(2\pi)^3 M_A} \int \sin\theta_l d\theta_l \int \sin\theta_p d\theta_p p f_{rec}^{-1} \sigma_M^{Z,W^\pm} \\ &\quad \times [v_L R_L + v_T R_T + h v_T' R_T'], \end{aligned} \tag{130}$$

where θ_l denotes the scattering angle of the lepton and $h = -1$ ($h = +1$) corresponds to the helicity of the incident ν ($\bar{\nu}$). The squared four-momentum transfer is given by $Q^2 = q^2 - \omega^2 = -q_\mu^2$. For the NC reaction, σ_M^Z is defined by

$$\sigma_M^Z = \left(\frac{G_F \cos(\theta_l/2) E_f M_Z^2}{\sqrt{2}\pi (Q^2 + M_Z^2)} \right), \tag{131}$$

and for the CC reaction

$$\sigma_M^{W^\pm} = \sqrt{1 - \frac{M_l^2}{E_f}} \left(\frac{G_F \cos(\theta_C) E_f M_W^2}{2\pi (Q^2 + M_W^2)} \right)^2, \tag{132}$$

where M_Z and M_W are the rest mass of Z-boson and W-boson, respectively. θ_C denotes the Cabibbo angle given by $\cos^2\theta_C \simeq 0.9749$. The recoil factor f_{rec} is given as

$$f_{rec} = \frac{E_{A-1}}{M_A} \left| 1 + \frac{E_p}{E_{A-1}} \left[1 - \frac{\mathbf{q}\cdot\mathbf{p}}{p^2} \right] \right|. \tag{133}$$

For the NC reaction, the kinematical coefficients v are given by

$$v_L = 1, \qquad v_T = \tan^2\frac{\theta_l}{2} + \frac{Q^2}{2q^2}, \qquad v'_T = \tan\frac{\theta_l}{2}\left[\tan^2\frac{\theta_l}{2} + \frac{Q^2}{q^2}\right]^{1/2}, \quad (134)$$

and corresponding response functions are expressed as

$$R_L = \left|J^0 - \frac{\omega}{q}J^z\right|^2, \qquad R_T = |J^x|^2 + |J^y|^2, \qquad R'_T = 2\mathrm{Im}(J^{x*}J^y). \quad (135)$$

For the CC reaction, the coefficients v are given by

$$\begin{aligned}
v_L^0 &= 1 + \sqrt{1 - \frac{M_l^2}{E_f^2}}\cos\theta_l, \\
v_L^z &= 1 + \sqrt{1 - \frac{M_l^2}{E_f^2}}\cos\theta_l - \frac{2E_iE_f}{q^2}\left(1 - \frac{M_l^2}{E_f^2}\right)\sin^2\theta_l, \\
v_L^{0z} &= \frac{\omega}{q}\left(1 + \sqrt{1 - \frac{M_l^2}{E_f^2}}\cos\theta_l\right) + \frac{M_l^2}{E_fq}, \\
v_T &= 1 - \sqrt{1 - \frac{M_l^2}{E_f^2}}\cos\theta_l + \frac{E_iE_f}{q^2}\left(1 - \frac{M_l^2}{E_f^2}\right)\sin^2\theta_l, \\
v'_T &= \frac{E_i + E_f}{q}\left(1 - \sqrt{1 - \frac{M_l^2}{E_f^2}}\cos\theta_l\right) - \frac{M_l^2}{E_fq}.
\end{aligned} \quad (136)$$

The corresponding response functions are given by

$$\begin{aligned}
R_L^0 &= |J^0|^2, \qquad R_L^z = |J^z|^2, \qquad R_L^{0z} = -2\mathrm{Re}(J^0J^{z*}), \\
R_T &= |J^x|^2 + |J^y|^2, \qquad\qquad R'_T = 2\mathrm{Im}(J^xJ^{y*}),
\end{aligned} \quad (137)$$

and

$$v_LR_L = v_L^0R_L^0 + v_L^zR_L^z + v_L^{0z}R_L^{0z}. \quad (138)$$

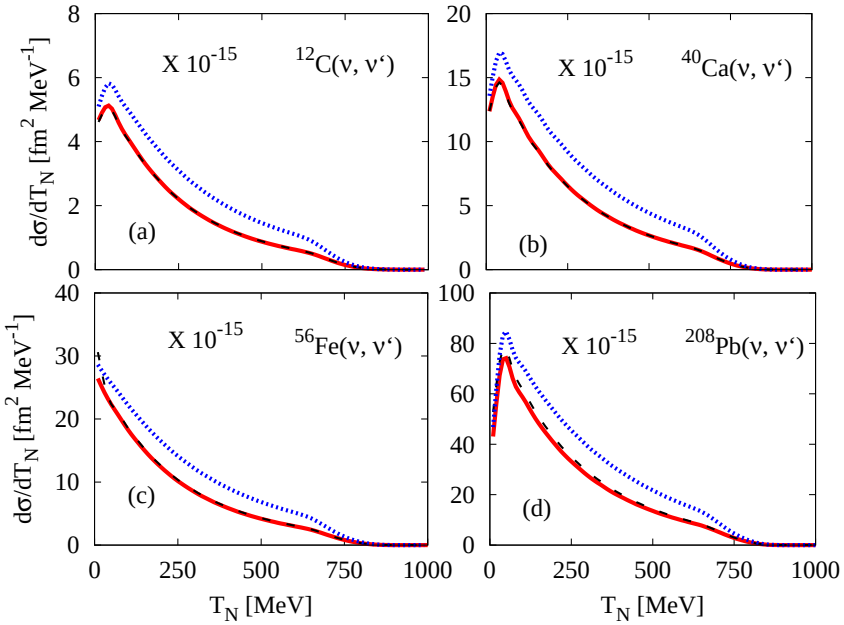

FIG. 20: (Color online) The differential cross sections of the NC $\nu - A$ scattering from ^{12}C, ^{40}Ca, ^{56}Fe, and ^{208}Pb.

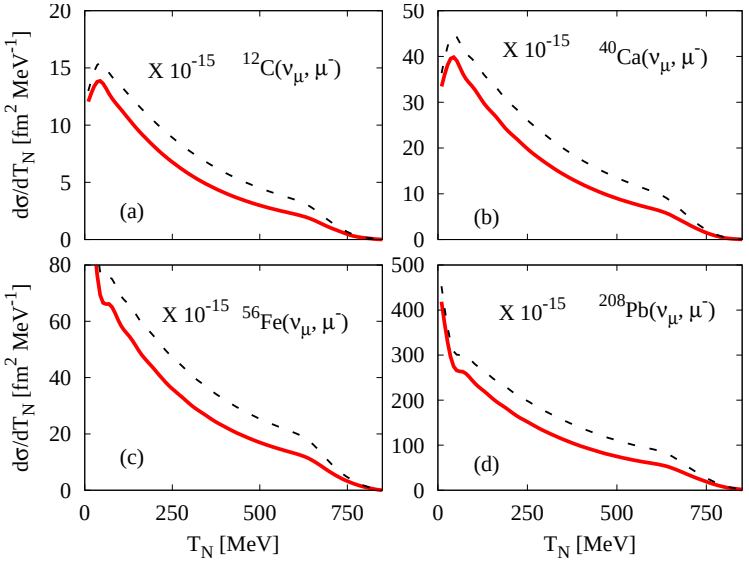

FIG. 21: (Color online) The differential cross sections of the CC $\nu - A$ scattering from ^{12}C, ^{40}Ca, ^{56}Fe, and ^{208}Pb.

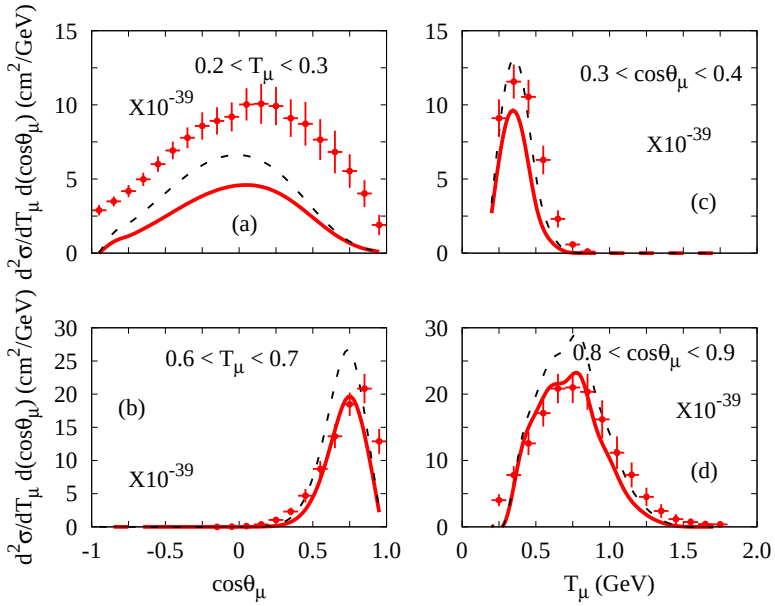

FIG. 22: (Color online) The double differential cross sections of the CC $\nu - A$ scattering in terms of the kinetic energy and the scattering angle of the outgoing muon. The experimental data were measured from MiniBooNE.

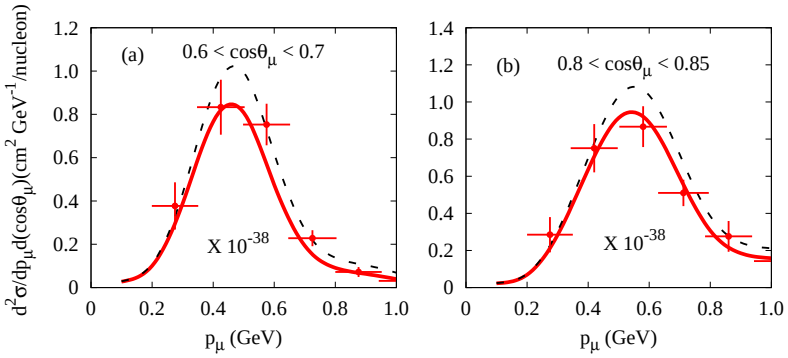

FIG. 23: (Color online) The flux integrated double differential cross sections in terms of incident muon momentum at fixed angle. The experimental data were measured from T2K.

In order to investigate the strangeness, the ratios between the NC and CC reactions are given by

$$R_{NC/CC} = \frac{\sigma(\nu, \nu' p)}{\sigma(\nu, \mu^- p)} = \frac{\sigma^{\nu p}_{NC}}{\sigma^{\nu}_{CC}},$$

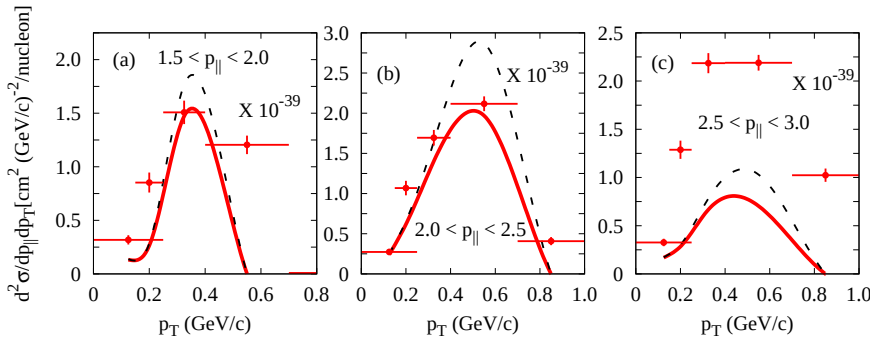

FIG. 24: (Color online) The double differential cross sections versus muon transverse momentum at fixed muon longitudinal momentum. The experimental data were measured from MINERν.

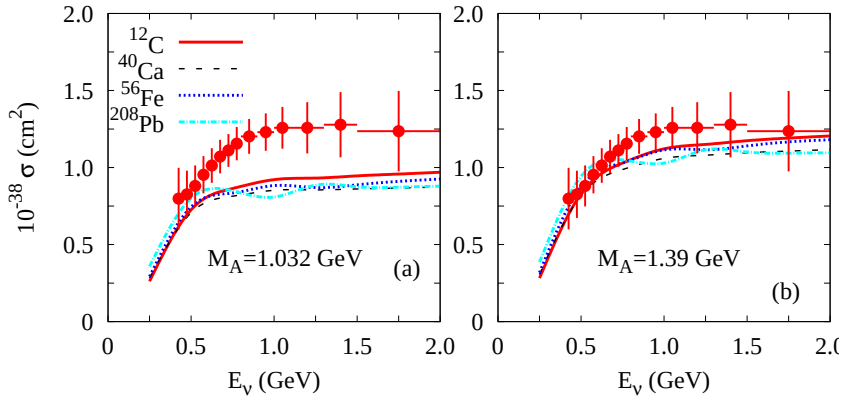

FIG. 25: (Color online) The total scaled cross sections of CC $\nu - A$ scattering in terms of the incident neutrino energies. The experimental data were measured from MiniBooNE.

$$\bar{R}_{NC/CC} = \frac{\sigma(\bar{\nu}, \bar{\nu}' n)}{\sigma(\bar{\nu}, \mu^+ n)} = \frac{\sigma_{NC}^{\bar{\nu}n}}{\sigma_{CC}^{\bar{\nu}}}. \tag{139}$$

Since the CC reaction is independent of isospin and the strangeness, and other possible effects of the nuclear structure could be cancelled out, these ratios are useful for probing the strangeness in the nuclei.

We introduce another definition of the ratios by focusing on the nucleon inside the target nucleus as follows:

$$R'_{NC/CC} = \frac{\sigma(\nu, \nu' n)}{\sigma(\nu, \mu^- p)} = \frac{\sigma_{NC}^{\nu n}}{\sigma_{CC}^{\nu}},$$

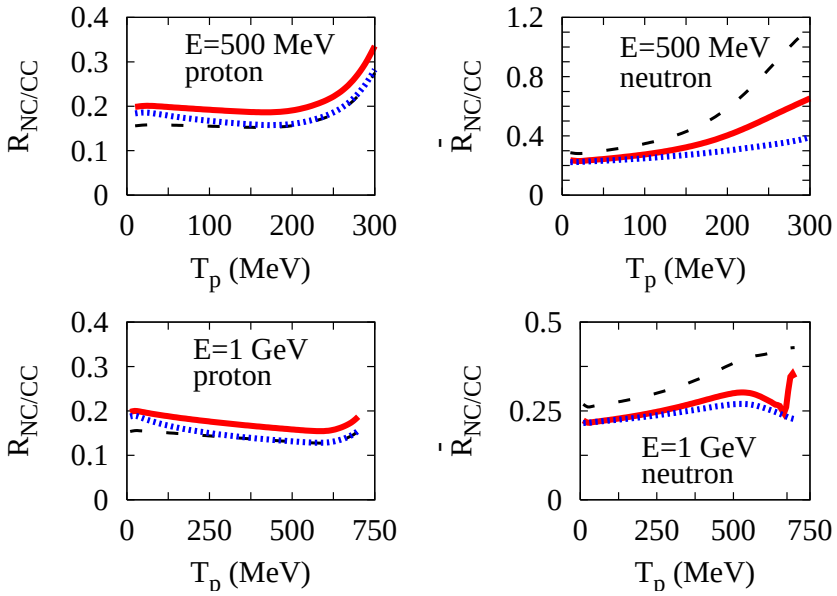

FIG. 26: (Color online)The ratio of the NC to the CC cross sections of neutrino-nucleus scattering for ^{12}C as a function of the knocked-out nucleon kinetic energy. For the NC reaction, solid (red) curves represent the results with $g_A^s = -0.19$ and $\mu_s = -0.4$, dashed (black) lines are with $g_A^s = 0.0$ and $\mu_s = -0.4$, and dotted (blue) lines are with $g_A^s = -0.19$ and $\mu_s = +0.4$.

$$\bar{R}'_{NC/CC} = \frac{\sigma(\bar{\nu}, \bar{\nu}' p)}{\sigma(\bar{\nu}, \mu^+ n)} = \frac{\sigma^{\bar{\nu}p}_{NC}}{\sigma^{\bar{\nu}}_{CC}}. \tag{140}$$

As another method to measure the effect of the strangeness, we introduce asymmetries by differences of the ν and $\bar{\nu}$ scattering cross sections via NC and CC reactions

$$A^p_{NC/CC} = \frac{\sigma^{\nu p}_{NC} - \sigma^{\bar{\nu}p}_{NC}}{\sigma^{\nu}_{CC} - \sigma^{\bar{\nu}}_{CC}}, \tag{141}$$

$$A^n_{NC/CC} = \frac{\sigma^{\nu n}_{NC} - \sigma^{\bar{\nu}n}_{NC}}{\sigma^{\nu}_{CC} - \sigma^{\bar{\nu}}_{CC}}. \tag{142}$$

Since nominators (denominators) contain only magnetic and axial form factors with (without) strangeness for a given proton or neutron, it is more

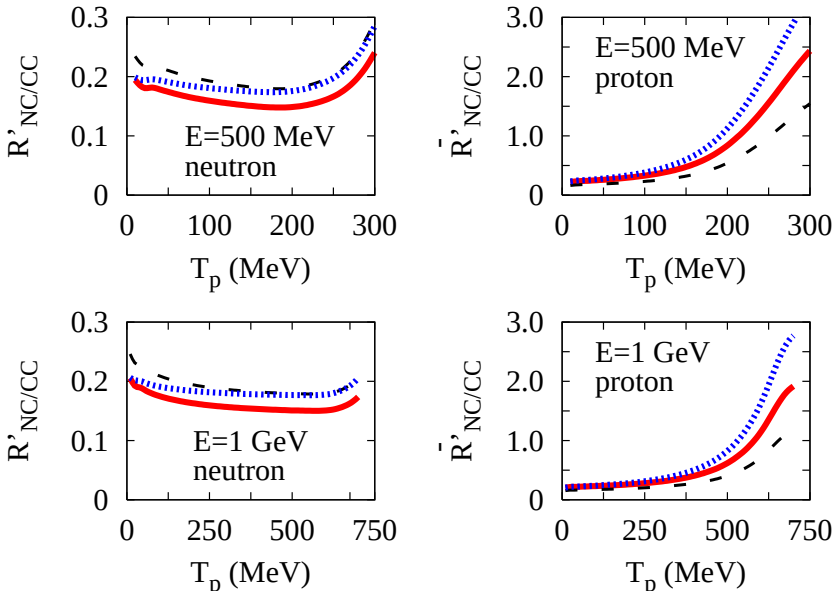

FIG. 27: (Color online)The ratio of the NC to the CC cross sections of neutrino-nucleus scattering for ^{12}C as a function of the knocked-out nucleon kinetic energy. For the NC reaction, solid (red) curves represent the results with $g_A^s = -0.19$ and $\mu_s = -0.4$, dashed (black) lines are with $g_A^s = 0.0$ and $\mu_s = -0.4$, and dotted (blue) lines are with $g_A^s = -0.19$ and $\mu_s = +0.4$.

useful for probing the effect of the strange quark contents in nuclei rather than the previous ratios.

♦ Comparison of structure functions for lepton-nucleus scattering

To extract the structure functions for the neutral-current reaction, the same method as the electron scattering is used as follows:

$$\frac{\sigma(+h) + \sigma(-h)}{2K} = v_L S_L + v_T S_T, \tag{143}$$

where σ denotes the differential cross section and $K = 4\pi^2 \frac{M_N M_{A-1}}{(2\pi)^3 M_A} p f_{rec}^{-1} \sigma_M^{Z,\,W^\pm}$ denotes the kinematics factor in front of integration in Eq. (130) with the

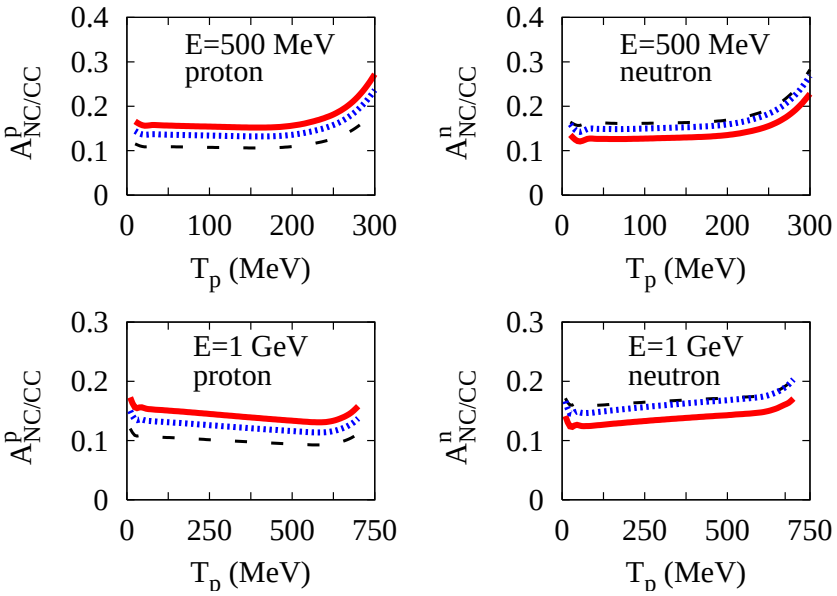

FIG. 28: (Color online)The ratio of the asymmetries between the NC and CC cross sections of neutrino-nucleus scattering for ^{12}C as a function of the knocked-out nucleon kinetic energy. For the NC reaction, solid (red) curves represent the results with $g_A^s = -0.19$ and $\mu_s = -0.4$, dashed (black) lines are with $g_A^s = 0.0$ and $\mu_s = -0.4$, and dotted (blue) lines are with $g_A^s = -0.19$ and $\mu_s = +0.4$.

recoil factor $f_{rec}^{-1} \sim 1$. The transverse structure function S_T becomes slope in term of variable v_T and the intercept point is S_L by keeping q and ω fixed because of $v_L = 1$.

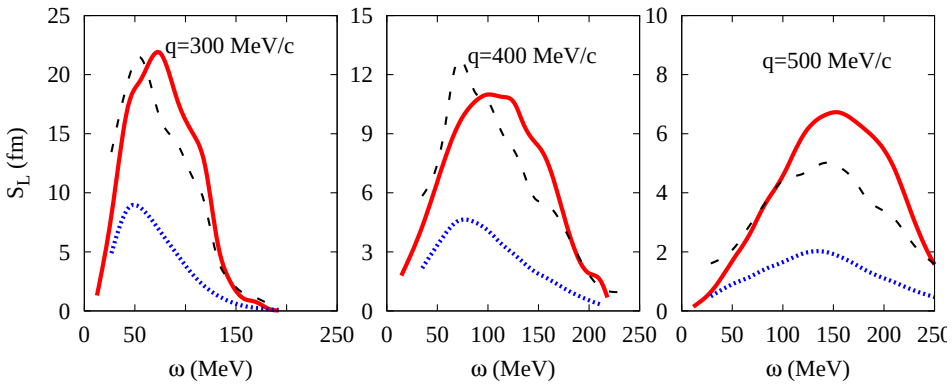

FIG. 29: (Color online) The solid curves are the results for the electron scattering, the dashed lines are for the NC neutrino scattering, and the dotted lines are without an axial form factor of the NC neutrino scattering.

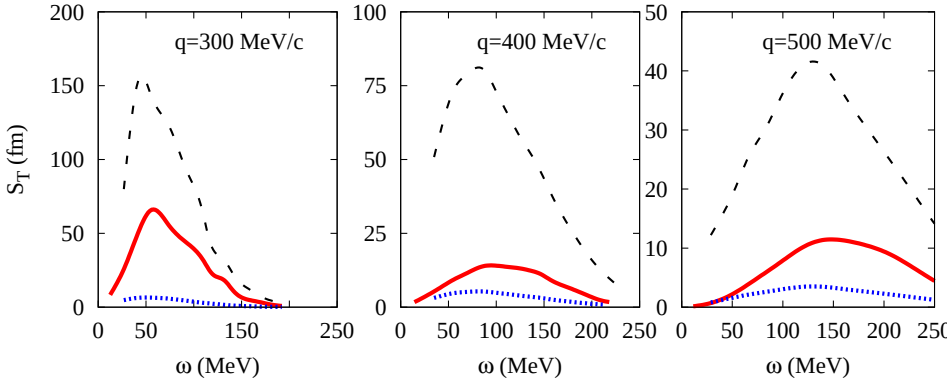

FIG. 30: (Color online) The solid curves are the results for the electron scattering, the dashed lines are for the NC neutrino scattering, and the dotted lines are without an axial form factor of the NC neutrino scattering.

Appendix : Reduced Matrix Elements of Multipole Operators

The following angular matrix elements are needed to evaluate the transition matrix element. The matrix element for the spin angle function can be written by

$$\langle \kappa'\mu'|\hat{O}|\kappa\mu\rangle = \int \chi^{\kappa'}_{\mu'}(\hat{r})^{\dagger}\hat{O}\chi^{\kappa}_{\mu}(\hat{r})d\Omega \tag{144}$$

for any operator $\hat{O}$.

The matrix element about a spherical harmonic operator becomes

$$\begin{aligned}\langle\kappa'\mu'|Y_L^M|\kappa\mu\rangle &= \int \chi_{\mu'}^{\kappa'}(\hat{r})^\dagger Y_L^M(\hat{r})\chi_\mu^\kappa(\hat{r})d\Omega \\ &= \langle j\mu, LM|j'\mu'\rangle\langle\kappa'\|Y_L^M\|\kappa\rangle \end{aligned} \tag{145}$$

where the double-bar matrix element is called the reduced matrix element. It is independent on the magnetic quantum numbers and is given by

$$\begin{aligned} I_L(\kappa',\kappa) &= \langle\kappa'\|Y_L^M\|\kappa\rangle \\ &= (-1)^{j+j'-L-1}\sqrt{\frac{(2j+1)(2L+1)}{4\pi(2j'+1)}}\langle j\frac{1}{2}, L0|j'\frac{1}{2}\rangle. \end{aligned} \tag{146}$$

The other multipole matrix elements with Dirac spinor become

$$\langle\kappa'\mu'|\boldsymbol{\sigma}\cdot\mathbf{Y}_{L\,L}^M|\kappa\mu\rangle = \frac{\kappa-\kappa'}{\sqrt{L(L+1)}}\langle\kappa'\mu'|Y_L^M|\kappa\mu\rangle \tag{147}$$

$$\langle\kappa'\mu'|\boldsymbol{\sigma}\cdot\mathbf{Y}_{L\,L-1}^M|\kappa\mu\rangle = \frac{\kappa'+\kappa-L}{\sqrt{L(2L+1)}}\langle\kappa'\mu'|Y_L^M|-\kappa\mu\rangle \tag{148}$$

$$\langle\kappa'\mu'|\boldsymbol{\sigma}\cdot\mathbf{Y}_{L\,L+1}^M|\kappa\mu\rangle = \frac{\kappa'+\kappa+L+1}{\sqrt{(L+1)(2L+1)}}\langle\kappa'\mu'|Y_L^M|-\kappa\mu\rangle. \tag{149}$$

The reduced matrix elements for vetor spherical harmonic operator and spin operator are given by

$$\langle\kappa'\mu'\|\boldsymbol{\sigma}\cdot\mathbf{Y}_{L\,L}^M\|\kappa\mu\rangle = \frac{\kappa-\kappa'}{\sqrt{L(L+1)}}I_L(\kappa',\kappa) \tag{150}$$

$$\langle\kappa'\mu'\|\boldsymbol{\sigma}\cdot\mathbf{Y}_{L\,L-1}^M\|\kappa\mu\rangle = \frac{\kappa'+\kappa-L}{\sqrt{L(2L+1)}}I_L(\kappa',-\kappa) \tag{151}$$

$$\langle\kappa'\mu'\|\boldsymbol{\sigma}\cdot\mathbf{Y}_{L\,L+1}^M\|\kappa\mu\rangle = \frac{\kappa'+\kappa+L+1}{\sqrt{(L+1)(2L+1)}}I_L(\kappa',-\kappa). \tag{152}$$

In evaluating the transition amplitude, we need the following multiple analysis relationship;

$$\langle\psi_p|\boldsymbol{\gamma}\cdot\mathbf{Y}_{L\,L}^M|\psi_b\rangle = \int {\psi_p}^\dagger\boldsymbol{\gamma}\cdot\mathbf{Y}_{L\,L}^M\psi_b d\Omega_r$$

$$
\begin{aligned}
&= \frac{i(\kappa_b+\kappa_p)}{\sqrt{L(L+1)}}(-f_{\kappa_p}g_{\kappa_b}+g_{\kappa_p}f_{\kappa_b}) \\
&\times \langle j_b\mu_b, LM|j_p\mu_p\rangle I_L(\kappa_p,-\kappa_b) \qquad (153)
\end{aligned}
$$

$$
\begin{aligned}
\langle\psi_p|\boldsymbol{\alpha}\cdot\mathbf{Y}^M_{L\,L}|\psi_b\rangle &= \int {\psi_p}^\dagger\boldsymbol{\alpha}\cdot\mathbf{Y}^M_{L\,L}\psi_b d\Omega_r \\
&= \frac{i(\kappa_b+\kappa_p)}{\sqrt{L(L+1)}}(-f_{\kappa_p}g_{\kappa_b}-g_{\kappa_p}f_{\kappa_b}) \\
&\times \langle j_b\mu_b, LM|j_p\mu_p\rangle I_L(\kappa_p,-\kappa_b) \qquad (154)
\end{aligned}
$$

$$
\begin{aligned}
\langle\psi_p|\gamma^0\boldsymbol{\Sigma}\cdot\mathbf{Y}^M_{L\,L}|\psi_b\rangle &= \int {\psi_p}^\dagger\gamma^0\boldsymbol{\Sigma}\cdot\mathbf{Y}^M_{L\,L}\psi_b d\Omega_r \\
&= \frac{\kappa_b-\kappa_p}{\sqrt{L(L+1)}}(f_{\kappa_p}f_{\kappa_b}+g_{\kappa_p}g_{\kappa_b}) \\
&\times \langle j_n\mu_b, LM|j_p\mu_p\rangle I_L(\kappa_p,\kappa_b) \qquad (155)
\end{aligned}
$$

$$
\begin{aligned}
\langle\psi_p|\boldsymbol{\alpha}\cdot\mathbf{Y}^M_{L\,L-1}|\psi_b\rangle &= \int {\psi_p}^\dagger\boldsymbol{\alpha}\cdot\mathbf{Y}^M_{L\,L-1}\psi_b d\Omega_r \\
&= \frac{i}{\sqrt{L(2L+1)}}[(\kappa_p-\kappa_b)(f_{\kappa_p}g_{\kappa_b}+g_{\kappa_p}f_{\kappa_b}) \\
&- L(f_{\kappa_p}g_{\kappa_b}-g_{\kappa_p}f_{\kappa_b})] \\
&\times \langle j_b\mu_b, LM|j_p\mu_p\rangle I_L(\kappa_p,\kappa_b) \qquad (156)
\end{aligned}
$$

$$
\begin{aligned}
\langle\psi_p|\boldsymbol{\gamma}\cdot\mathbf{Y}^M_{L\,L-1}|\psi_b\rangle &= \int {\psi_p}^\dagger\boldsymbol{\gamma}\cdot\mathbf{Y}^M_{L\,L-1}\psi_b d\Omega_r \\
&= \frac{i}{\sqrt{L(2L+1)}}[(\kappa_p-\kappa_b)(f_{\kappa_p}g_{\kappa_b}-g_{\kappa_p}f_{\kappa_b}) \\
&- L(f_{\kappa_p}g_{\kappa_b}+g_{\kappa_p}f_{\kappa_b})]\langle j_b\mu_b, LM|j_p\mu_p\rangle \\
&\times I_L(\kappa_p,\kappa_b) \qquad (157)
\end{aligned}
$$

$$\begin{aligned}\langle\psi_p|\gamma^0\boldsymbol{\Sigma}\cdot\mathbf{Y}^M_{L\,L-1}|\psi_b\rangle &= \int {\psi_p}^\dagger\gamma^0\boldsymbol{\Sigma}\cdot\mathbf{Y}^M_{L\,L-1}\psi_b d\Omega_r \\ &= \frac{1}{\sqrt{L(2L+1)}}[(\kappa_p+\kappa_b)(f_{\kappa_p}f_{\kappa_b}+g_{\kappa_p}g_{\kappa_b}) \\ &- L(f_{\kappa_p}f_{\kappa_b}-g_{\kappa_p}g_{\kappa_b})] \\ &\times \langle j_b\mu_b, LM|j_p\mu_p\rangle I_L(\kappa_p,-\kappa_b) \qquad (158)\end{aligned}$$

$$\begin{aligned}\langle\psi_p|\boldsymbol{\alpha}\cdot\mathbf{Y}^M_{L\,L+1}|\psi_b\rangle &= \int {\psi_p}^\dagger\boldsymbol{\alpha}\cdot\mathbf{Y}^M_{L\,L+1}\psi_b d\Omega_r \\ &= \frac{i}{\sqrt{(L+1)(2L+1)}}[(\kappa_p-\kappa_b)(f_{\kappa_p}g_{\kappa_b}+g_{\kappa_p}f_{\kappa_b}) \\ &+ (L+1)(f_{\kappa_p}g_{\kappa_b}-g_{\kappa_p}f_{\kappa_b})] \\ &\times \langle j_b\mu_b, LM|j_p\mu_p\rangle I_L(\kappa_p,\kappa_b) \qquad (159)\end{aligned}$$

$$\begin{aligned}\langle\psi_p|\boldsymbol{\gamma}\cdot\mathbf{Y}^M_{L\,L+1}|\psi_b\rangle &= \int {\psi_p}^\dagger\boldsymbol{\gamma}\cdot\mathbf{Y}^M_{L\,L+1}\psi_b d\Omega_r \\ &= \frac{i}{\sqrt{(L+1)(2L+1)}}[(\kappa_p-\kappa_b)(f_{\kappa_p}g_{\kappa_b}-g_{\kappa_p}f_{\kappa_b}) \\ &+ (L+1)(f_{\kappa_p}g_{\kappa_b}+g_{\kappa_p}f_{\kappa_b})] \\ &\times \langle j_b\mu_b, LM|j_p\mu_p\rangle I_L(\kappa_p,\kappa_b) \qquad (160)\end{aligned}$$

$$\begin{aligned}\langle\psi_p|\gamma^0\boldsymbol{\Sigma}\cdot\mathbf{Y}^M_{L\,L+1}|\psi_b\rangle &= \int {\psi_p}^\dagger\gamma^0\boldsymbol{\Sigma}\cdot\mathbf{Y}^M_{L\,L+1}\psi_b d\Omega_r \\ &= \frac{1}{\sqrt{(L+1)(2L+1)}}[(\kappa_p+\kappa_b)(f_{\kappa_p}f_{\kappa_b}+g_{\kappa_p}g_{\kappa_b}) \\ &+ (L+1)(f_{\kappa_p}f_{\kappa_b}-g_{\kappa_p}g_{\kappa_b})] \\ &\times \langle j_b\mu_b, LM|j_p\mu_p\rangle I_L(\kappa_p,-\kappa_b). \qquad (161)\end{aligned}$$